Aalto-yliopisto
Aalto-universitetet
Aalto University

Master's Program in Water and Environmental Engineering

Projection and Adaptation to Future Coastal Erosion in Vietnam

Ville Vanhanen

Master's thesis
2024

Aalto-yliopisto
Aalto-universitetet
Aalto University

Author Ville Vanhanen

Title of thesis Projection and Adaptation to Future Coastal Erosion in Vietnam

Programme Water and Environmental Engineering

Major Water and Environmental Engineering

Thesis supervisor Associate Prof. Matti Kummu, Aalto University

Date 30.08.2024 **Number of pages** 49 **Language** English

Abstract

One of the most severe issues worldwide is the beach loss caused by sea level rise (SLR). The repercussions of SLR-driven beach losses along the Vietnamese coastline may be severe due to Vietnam's dense population and important economy zone along the said coastline. This study gathered sandy beaches along the Vietnamese coast to gain a better understanding of the future beach loss situation due to SLR. Future SLR projection dataset (CMIP6, IPCC) was used, along with the Bruun rule, to project the future beach loss along the Vietnamese coastline. The main findings of this study are the following: (1) The total beach length along the Vietnamese coastline is 1330.1 km which is 40.8% of the total coastline length. This study found that Quang Binh, Ha Tinh and Binh Thuan provinces have got the most account of sandy beaches area-wise, with 13%, 13% and 11% respectively. (2) The worst-case projections along the Vietnamese coasts show a future beach loss of 67% and 70.6 km^2 out of the total beach area of 105.4 km^2 for the SSP5-8.5 scenario in CMIP6. Severe beach losses of more than 90% are projected along the South Central coast provinces. (3) According to the Coastal Vulnerability Index (CVI) done to the whole coastline of Vietnam against SLR, the coastal vulnerability will increase or stay the same along the entire Vietnamese coastline.

Overall, the future beach loss projections in Vietnam are around the same magnitude as in other studies done to China, Japan and Thailand before.

Keywords Sea level rise, sandy beach, Bruun rule, shoreline retreat, beach loss, Coastal Vulnerability Index (CVI)

Aalto-yliopisto
Aalto-universitetet
Aalto University

Tekijä Ville Vanhanen

Työn nimi Projisointi ja sopeutuminen tulevaan rannikkoeroosioon Vietnamissa

Koulutusohjelma Vesi- ja ympäristötekniikka

Pääaine Water and Environmental Engineering

Vastuuopettaja/valvoja Associate Prof. Matti Kummu, Aalto yliopisto

Päivämäärä 30.08.2024 **Sivumäärä** 49 **Kieli** Englanti

Tiivistelmä

Rantaviivan muutos merenpinnan nousun takia on yksi vakavimmista ongelmista maailmanlaajuisesti. Merenpinnan nousun aiheuttaman rantaviivan muutoksen seuraukset Vietnamin rannikolla voivat olla vakavia, koska väestöntiheys on rannikolla suuri ja rannikkoalue on myös tärkeä taloudellisesti. Tässä tutkimuksessa kerättiin tietoa Vietnamin rannikon hiekkarannoista, jota käytettiin selvittämään hiekkarantojen rantaviivan muutosta tulevaisuudessa. Tutkimuksessa käytettiin tulevaisuuden merenpinnan nousun ennustedataa (CMIP6, IPCC) sekä Bruunin sääntöä, joiden avulla arvioitiin Vietnamin rantaviivan muutosta tulevaisuudessa. Tutkimuksen pääasialliset havainnot ovat seuraavat: (1) Vietnamin rannikon hiekkarantojen kokonaispituus on 1330,1 km, joka on 40,8 % koko rannikon pituudesta. Tutkimuksessa havaittiin, että Quang Binh, Ha Tinh ja Binh Thuan maakunnissa on eniten hiekkarantoja suhteessa rantojen kokonaispinta-alaan, 13 %, 13 % ja 11 % osuuksilla. (2) Pahimmat ennusteet Vietnamin rannikolle osoittavat 67 % ja 70,6 km^2 rantaviivan muutosta 105.4 km^2 kokonaispinta-alasta SSP5-8.5-skenaariossa CMIP6 simulaatioissa. Vakavaa eli yli 90 % rantaviivan muutosta ennustetaan Etelä-Keski-Vietnamin rannikkoalueille. (3) Koko Vietnamin rannikolle tehdyn rannanhaavoittuvuusindeksin mukaan rantahaavoittuvuus kasvaa tai pysyy samana koko Vietnamin rannikolla suhteessa merenpinnan nousuun.

Vietnamin rantaviivan arvioutu muutos tulevaisuudessa on samaa suuruusluokkaa kuin aiemmissa tutkimuksissa Kiinan, Japanin ja Thaimaan rantaviivan ennustettu muutos.

Avainsanat Merenpinnan nousu, hiekkaranta, Bruun rule, rantaviivan muutos, rantahaavoittuvuus indeksi

Table of contents

Preface and acknowledgements

I want to thank my Aalto University supervisor Professor Matti Kummu and Keiko Udo & Janaka Bamunawala from Tohoku University for their great advice and guidance.

Sendai, Japan August 30, 2024
Ville Vanhanen

Symbols and abbreviations

Abbreviations

SLR	Sea level rise
AGP	Arc GIS Pro
CVI	Coastal Vulnerability Index
SSP	Shared Socioeconomic Pathways
RCP	Representative Concentration Pathway

1 Introduction

Sandy beaches are among the most important resources in coastal areas as they provide recreational opportunities which in turn, greatly benefit coastal cities in terms of economic and environmental aspects. (Somphong et al., 2020). The coastal areas globally are well developed and heavily populated, with 15 out of the 20 megacities with populations over 10 million located within them. (Luijendijk et al., 2018).

Coastal areas are extremely dynamic because of natural and human activities (Ritphring et al., 2021). According to previous studies, coastal areas are currently more prone to natural and human-made hazards that cause coastal erosion. This combined with climate change and other human activities can alter the natural processes of coasts which in turn could increase the risk of coastal erosion and coastal retreat. (Pang et al., 2023)

Hinkel et al. (2013) and Vousdoukas et al. (2020) estimated that up to 50% of the world's sandy beaches could face severe erosion, and that the global sandy beach loss could reach 17 000 km^2 by the end of the century. The Intergovernmental Panel on Climate Change (IPCC) projected a high rise in sea level at the end of the century on basis of different shared socioeconomic pathways (SSP) scenarios of CMIP6 (IPCC, 2021). This could further increase the risk of erosion to sandy beaches around the world.

Vietnam is the 16^{th} most populated country in the world with a population of 99.5 million people (2022), 48.6 million of whom live in the coastal provinces. The coastal provinces make up 41.4% of Vietnam's land area. The GDP per capita of coastal provinces was 4543 PPP US$ and coastal provinces made up approximately 60% of the total GDP of Vietnam in 2011. (GSO, 2024)

A report by the Ministry of Natural Resources and Environment (Vietnam) reported that the average sea level rose at all measuring stations at a rate of 2.45 mm/year between 1960 – 2014. For the period 1993 – 2014, the increase was 3.34 mm/year. Data acquired from satellites between 1993 - 2014 revealed that the average water level along coastal areas in Vietnam increased by 3.5±0.7 mm/year. (Monre, 2016).

Several studies have been conducted on coastal erosion in Vietnam. Duc et al. (2016) investigated the impacts of climate change on the large-scale erosion coast of the Hai Hau district in Nam Dinh Province. They used the Bruun rule to obtain the rate of erosion due to SLR, which in turn can be used to calculate the beach lowering rate. They reported that severe typhoons and SLR increase beach lowering, coastal erosion and scour. Furthermore, average waves during high tide can cause severe soil erosion and lead to dyke failure by 2060.

Vinh and Truong (2012) investigated the erosion situation of the Nga Bay River in Ho Chi Minh City. They collected soil and water samples, used remote sensing GIS methods to analyze changes in riverbanks and used a numerical model (MIKE 21) to calculate current velocities and wind-induced wave height-affected riverbanks. They reported that the erosion rate was approximately 10 m/y in the river. The main contributors to this were currents, waves and ship-generated waves, along with the human factor of destroying mangrove trees to reclaim salt ponds and shrimp ponds.

Thinh et al. (2018) researched the damage caused by beach erosion for tourism at Hoi, a world heritage site in Quang Nam Province. They adopted the digital shoreline analysis system (DSAS) to estimate the average coastal erosion rate. They reported that the main drivers of erosion were SLR along the Central Coast of Vietnam, the construction of hydropower dams in the Thu Bon and Vu Gia rivers and illegal sand mining in the South China Sea.

Nguyen et al. (2021) assessed coastal landscape vulnerability to erosion in tropical storms at regional and local scales in Vietnam. Machine learning has been used to identify different coastal structures along the Vietnamese coastline. They used principal criterion analysis (PCA) for CVI analysis at the national, regional and local scales. The findings of the present study are that more than 20% of the Vietnamese coastline has high CVI values and that storms have heavily affected coastal landscapes with residential and tourism lands close to beaches without protective forests.

The scale of the entire Vietnamese coastline, along with future erosion projections and adaptations, is new in this study compared with previous studies. This study aims to gather beach characteristics along the whole Vietnamese coastline and project beach loss due to SLR data provided by the AR6 report (IPCC, 2021). The characteristics of the projected beach loss along the Vietnamese coastline under the different SSP scenarios are further analyzed, and the adaptations measured are discussed.

Research has not been conducted before on the future erosion situation along the entire Vietnamese coastline, which is why this study was conducted. This study can help policy makers in Vietnam assess future needs for coastal protection measurements in coastal provinces.

2 Literature review

In coastal erosion, sand is moved from the shore and deposited somewhere else, for example, to another beach, the deeper ocean bottom, into an ocean trench or onto the landside of a dune. Sand being removed from the sand sharing system causes irreversible changes in the beach shape and structure. Its impact is usually not observed immediately, as it involves a tsunami or storm surge but gradually occurs over months or years; hence, it is generally classified as a “long-term coastal hazard”. (Prasad and Kumar, 2014).

Coastal erosion, the process by which coastlines are gradually worn away by the action of natural forces such as wave action, tidal currents, and human activities, has been a significant subject of study in the literature.
Many studies have investigated coastal erosion in coastal countries, such as China (Xiao et al., 2023), Japan (Udo and Takeda, 2017), Egypt (Sharaan and Udo, 2020) and Thailand (Ritphring et al., 2018).

High-energy waves can remove large amounts of sand during storms or high tides, which in turn affect the beach profile (narrower and steeper). Longshore waves approaching the beach at an angle can transport sand along the coast, resulting in erosion and deposition of sand in different areas. (Bird, 2008).

The tidal range affects the extent of wave action on a beach, which in turn affects erosion patterns. A large tidal range means that more of the beach is exposed to wave action, which can cause greater erosion. During large tidal range events (spring tides, storms), erosion ranges are usually greater as well. (Bird, 2008).

Storm surges combine high-energy waves and elevated water levels that can cause significant erosion by quickly removing large amounts of sand from a beach. The beach may need years to recover from such an event, and repeated storm surges can permanently change the beach’s morphology. (Bird, 2008).

Human activities, such as building infrastructure (seawall, groynes and jetties), can disturb natural sediment transport and thus increase the severity of erosion in certain areas. Seawalls protect the land behind them but at the cost of increasing erosion by reflecting wave energy back onto the beach. Jetties and groynes interrupt longshore sediment transport, which leads to sand accumulation and erosion on different sides of structures. (Schoonees et al., 2019).

Sand mining removes sand from beaches for construction purposes, which causes the beach elevation to decrease. This in turn increases the susceptibility of the beach to erosion. (Bird, 2008).

Beach nourishment, although intended for counteracting erosion, can have mixed results depending on the characteristics of the sand used. If the added sand’s sediment size does not match that of the beach, the added sand can be quickly eroded away and sometimes even accelerate the erosion process. (Bird, 2008).

Climate change increases SLR, storminess and changing wave patterns, which can lead to more severe and frequent erosion events. Furthermore, changes in temperature and precipitation patterns can affect sediment supply and vegetation, which may further increase erosion. (Bird, 2008).

Vegetation loss affects the stabilization of sandy beaches. Vegetation, especially dune plants, helps trap and stabilize sandy beaches against wave and wind action. Changes in wind action due to human activities or vegetation loss can lead to increased erosion of a sandy beach, as there is less to hold the sand in place. (Bird, 2008).

Descriptive studies and observational accounts were the primary focus of early coastal erosion. Gilbert's (1890) work on Lake Bonneville helped us understand the geomorphological processes shaping coastlines and laid the groundwork to better grasp the dynamic interactions between land and sea.

In the mid-20th century, Shepard's (1948) work on “Submarine Geology” gave us new insights into how underwater topography shapes coastal landscapes, and Bird's (1964) work "Coastal Geomorphology: An Introduction" classified coastal forms and the processes that affect them.

Currently, climate change is a major factor in coastal erosion, and emphasis has been placed on the impacts of SLR and extreme weather events. In addition to climate change, coastal erosion prediction and adaptation have also become important topics. (Pang et al., 2023).

Hard engineering solutions such as groins, jetties and seawalls were the focus of the work "Coasts in Crisis" by Williams et al. (1991). They noted that transferring the erosion problem downstream was one unintended problem of such structures. Furthermore, soft engineering solutions such as beach nourishment and dune stabilization were examined in

Carter's (1988) "Coastal Environments" book as more sustainable alternatives to hard engineering solutions. In their paper, Schoonees et al. (2019) discussed complementing hard structures with soft solutions or enhancing them with new nature-based adaptations in addition to hard structures for coastal protection.

The "Intergovernmental Panel on Climate Change (IPCC) Special Report on the Ocean and Cryosphere in a Changing Climate" (2019) discusses the vulnerability of coastal communities and the economic costs associated with erosion and sea-level rise. (IPCC, 2019). Moreover, "An Introduction to Coastal Zone Management" by Beatley et al. (2002) provides information on the management practices and policy frameworks aimed at mitigating erosion impacts.

There has been an emphasis on implementing physical, ecological and socioeconomic approaches to coastal erosion in recent studies. Bilkov et al. (2017) book about "Living Shoreline Design Guidelines for Shore Protection in Virginia's Estuarine Environments", state how this implementation can benefit coastal resilience.

Coastal erosion is a complex and multifaceted issue. The field currently contains a wide variety of perspectives, ranging from contemporary analyses to climate change impacts and human interventions. For the future management of coastal erosion, the continued integration of these different perspectives should continue.

3 Research material and methods

3.1 Vietnam's beach characteristics

There are 58 provinces in Vietnam, 28 of which are coastal provinces located next to the South China Sea (Figure 1). Vietnam's coastline is 3260 km long and spans from the northernmost coastal province, Quang Ninh, to the southernmost province, Ca Mau.

A "beach" was defined as the visible beach body enclosed by the continental area and the sea in this study (Ritphring et al., 2018). Beaches along the Vietnamese coastline were manually gathered via ArcGIS Pro (AGP) software (Figure 2). AGP uses Maxar satellite imagery as its baseline map, with a resolution of 0.5 m and an accuracy of 5 m. A total of 1390 beaches were identified and analyzed along the Vietnamese coastline in this study. The beaches were identified and extracted as polygons. "Minimum bounding geometry" (MBG), an AGP geoprocessing tool, was used to obtain an estimate of every beach alongside length, and the beach width was calculated by dividing the beach area by its alongside length. A tidal correction was performed to remove the tidal effects on the tide in the beach width by estimating the capture times of the satellite images in AGP (https://www.n2yo.com/satellite/?s=32060#results) and then checking the corresponding tide level at that time. Hourly datasets about the tide levels were downloaded from https://uhslc.soest.hawaii.edu/data/?rq#uh162a, and the data from the 4 tide stations were used to estimate the tide levels (Figure 3). The Qui Nhon station (1) had a recorded period of 11 years, and the average tide level was estimated by taking the average tide level across the recorded period (11 years). As some of the tide stations do not have enough data to estimate the average tidal levels, the Qui Nhon station's long recorded period was used to estimate the tide level for Hon Dau (3) and Vung Ang (4) stations. Coefficients were calculated by taking the average mean tide level for stations (3) and (4) and dividing it by the average tide level of station (1). The final tide levels for stations (3) and (4) were calculated by multiplying the (1) station's recorded mean tide level with the coefficients. The corrected beach width was calculated by first subtracting the mean sea level from the mean tide level and then dividing that value by the beach slope (tan α) and adding the new value to the original beach width value. The new value was positive for high tide and negative for low tide.

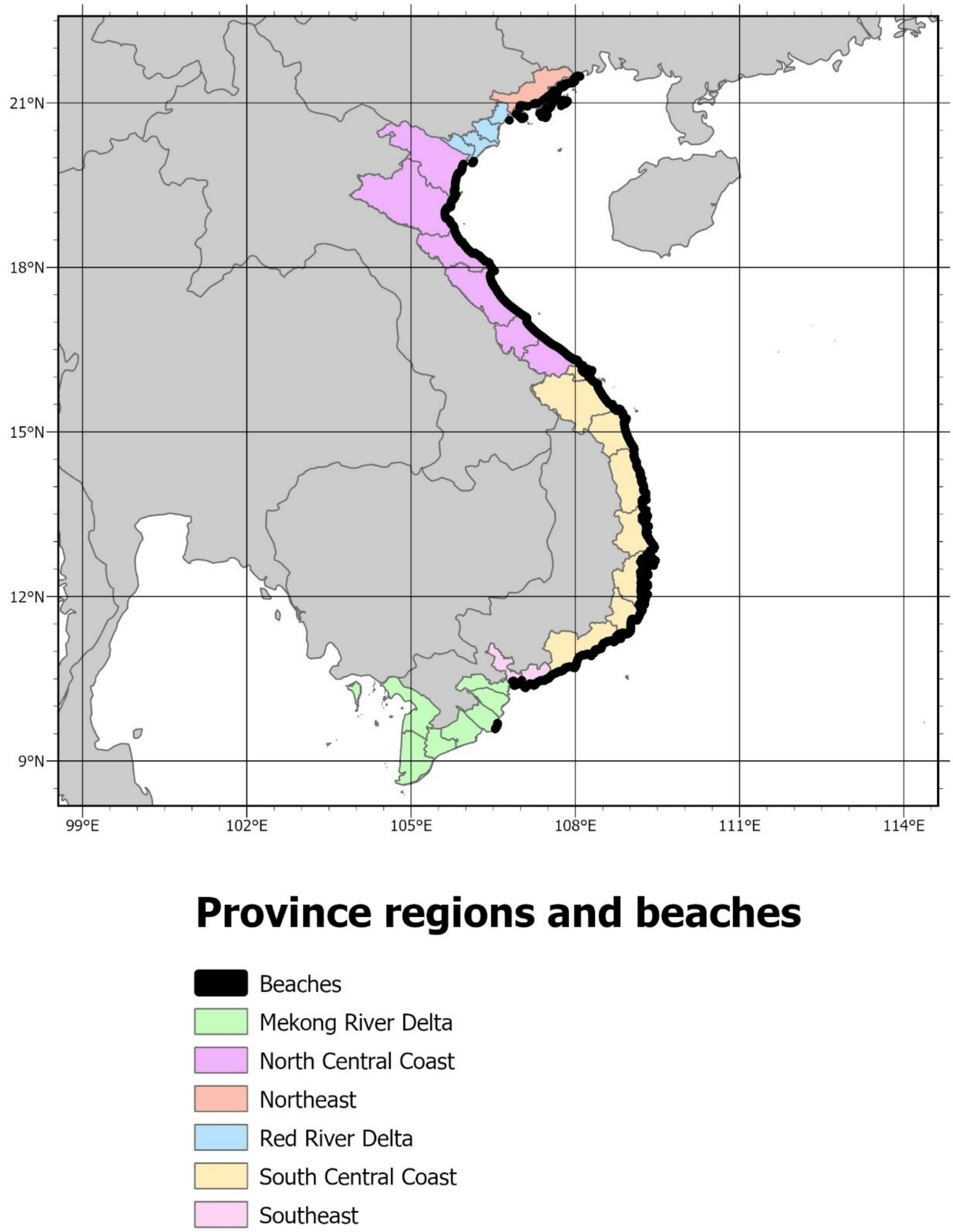

Figure 1 Beaches along the Vietnamese coastline and the regions of the 28 coastal provinces

Figure 2 Example of a polygonised beach in Dong Hoa district in Phu Yen Province.

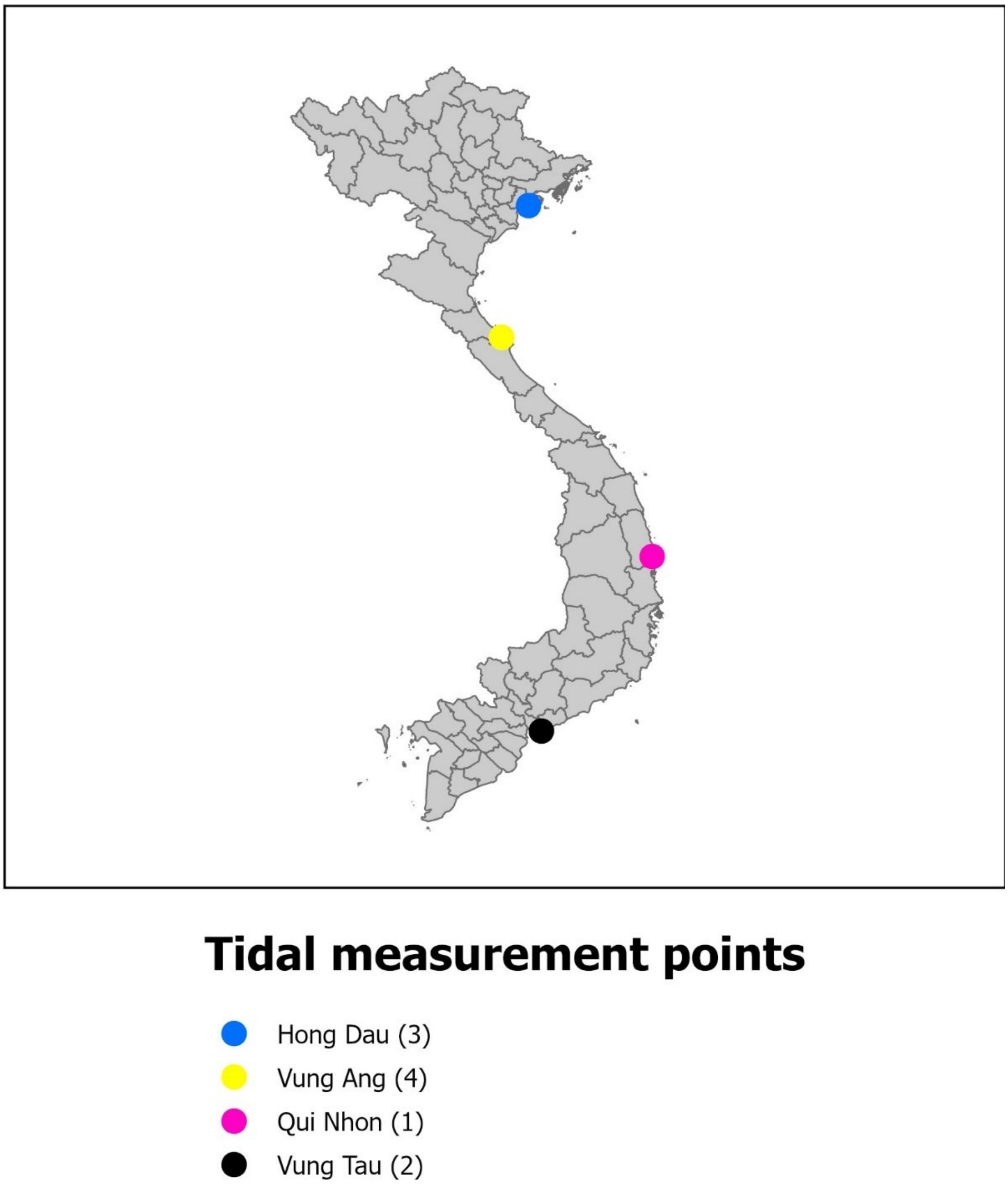

Figure 3 Tidal measurement points along the Vietnamese coast

The beach slope, tan(α), was obtained from the global database of coastal characteristics (GCC) dataset provided by Athanasiou et al. (2023). They gathered coastal slopes for ~730 000 cross-shore transects (with 1 km spacing between transects) along the global ice-free coastline. The coastal slope is defined and calculated as the slope between the depth of closure and the coastal maximum (first peak, as shown in Figure 18). Only values in the range of $0.01<slope<0.2$ were included. Otherwise, Wiegel's (1992) correlation between beach slope and sediment size, which is based on extensive field data and plotted relationship curves, could not be used to estimate the sediment size of slopes that are lower than 0.01 or greater than 0.2. The distribution of beach slopes is shown in Figure 4. Therefore, the sediment size was estimated by applying the relationship curves mentioned above, and the results are shown in Figure 4. The sediment size is between 0.2 and 0.4 mm for a large majority of the beaches, and larger values (greater than 0.6) can be found in the northern areas (northeast) and in the south central coast.

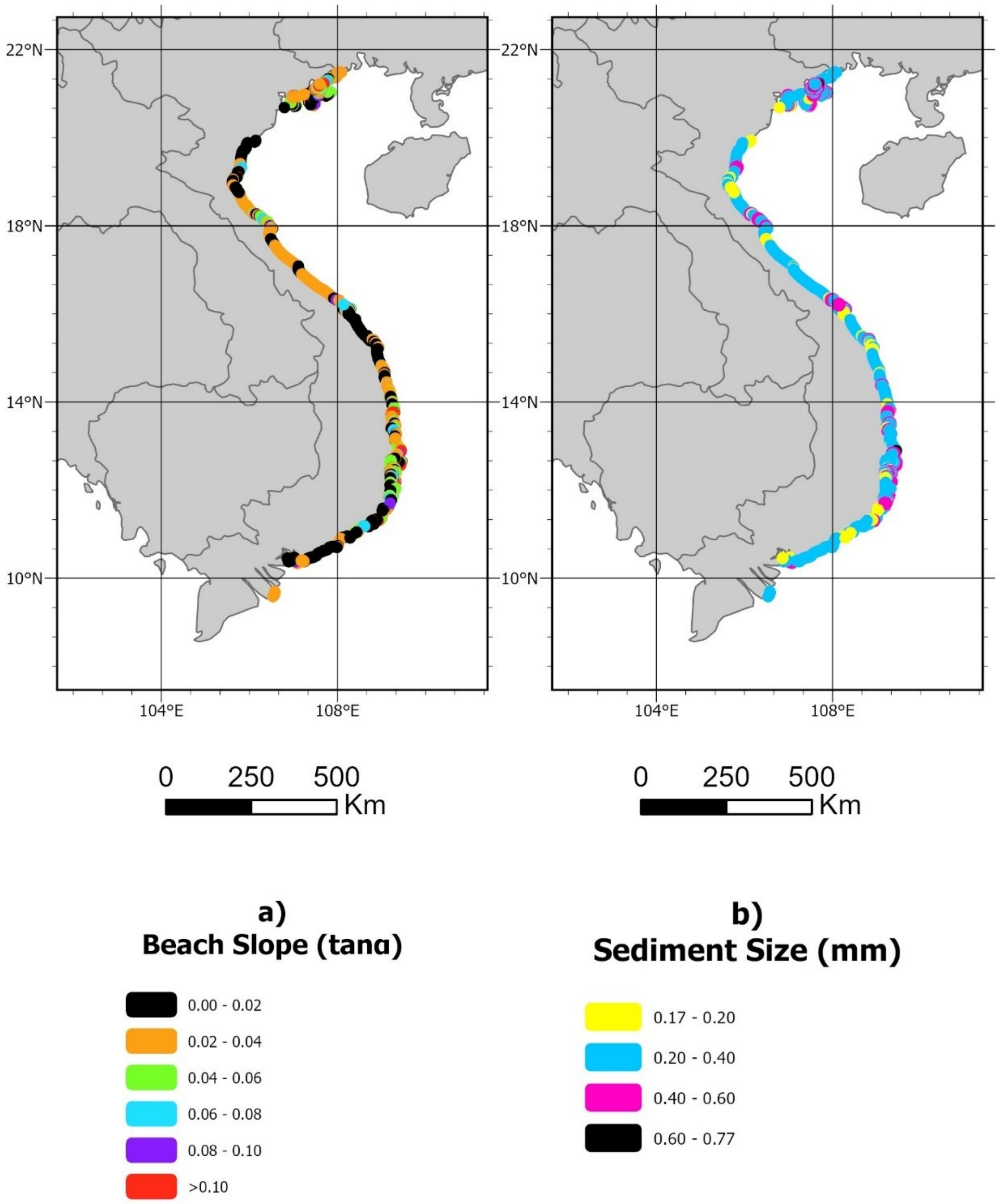

Figure 4 Beach slope and sediment size along the Vietnamese coast

3.2 The Bruun rule

The Bruun rule (1962) is a widely used method for projecting the future beach loss due to SLR. It assumes that the beach profile maintains its equilibrium shape by shifting upward and landward as the sea level rises (Figure 5). Sediment transportation from the foreshore to the seabed results in shoreline retreat.

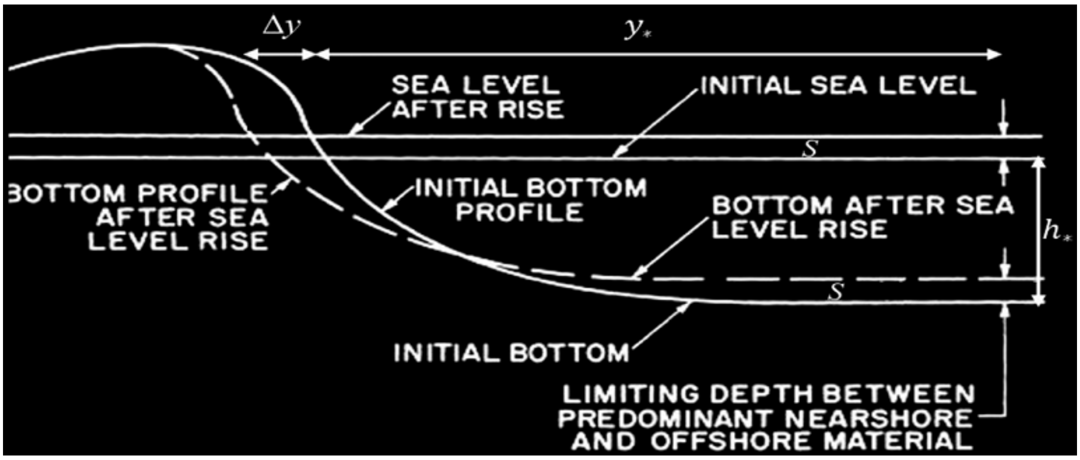

Figure 5 Beach response to SLR based on the Bruun rule (1962). The parameters are illustrated within the text.

The Bruun rule assumes that the beach profile, which is two-dimensional, maintains its equilibrium condition governed by equation (1)

$$h = Ay^{2/3} \tag{1}$$

where h is the water depth, A is the beach profile coefficient and y is the distance in the offshore direction. The slope values for each beach were used to estimate the sediment size for every beach on the basis of Wiegel (1992). The sediment size values were used to further estimate beach profile parameter A for every beach (U.S. Army Corps of Engineers, 2002). The shoreline retreat can be calculated via the following equation(2)

$$\frac{\Delta y}{y*} = -\frac{S}{(h_* + B_h)} \tag{2}$$

where Δy is the shoreline retreat, y* is the horizontal distance to the depth of closure which can be calculated from Eq. (3) using h_*, S is the sea level rise (SLR), h_* is the depth of closure and B_h is the berm height.

The depth of closure h_* can be calculated via the equation of Nicholls et al. (1996):

$$h_* = 2.28H_{\mathrm{e,t}} - 68.5\left(\frac{H_{e,t}^2}{gT_{e,t}^2}\right) \tag{3}$$

where $H_{e,t}$ is the nearshore significant wave height that exceeds 12 h per t years, $T_{e,t}$ is the associated wave period and g is the gravitational acceleration.

The berm height B_h can be estimated from the equation (4) by Takeda and Sunamura (1983):

$$B_h = 0.125H_b^{\frac{5}{8}} * (gT_s^2)^{\frac{3}{8}} \tag{4}$$

where H_b is the breaking wave height and T_s is the deep-water mean significant wave period. The breaking wave height H_b can be calculated via the equation (5) by Sunamura (1983):

$$\frac{H_b}{H_s} = (\tan\alpha)^{0.2} * \left(\frac{H_s}{L_s}\right)^{-0.25} \tag{5}$$

where H_s is the deep-water mean significant wave height, L_s is the deep-water mean significant wavelength and $\tan\alpha$ is the beach slope. The shoreline retreat caused by future SLR can be projected on the basis of beach characteristics (A and $\tan\alpha$), SLR data and wave data (H_s, T_s, $H_{e,t}$, $T_{e,t}$) as a result.

The future beach loss percentage for each sandy beach along the Vietnamese coastline was calculated by dividing Δy by the current beach width. The total sandy beach loss percentage for all of Vietnam was calculated by dividing the sandy beach loss area by the total sandy beach area. Furthermore, the shoreline retreat Δy was set at 100% if it exceeded the maximum beach width as the Bruun rule is not suitable for estimating shoreline retreat in non-beach areas.

This study considered only unprotected sandy beaches along the Vietnamese coastline.

3.3 Sea level and wave data

The regional SLR data used in this study was extracted from the IPCC 2021 AR6 report, which is a global scale projection based on different scenarios (IPCC, 2021). The scenarios used were SSP1-1.9, SSP1-2.6, SSP2-4.5, SSP3-7.0, and SSP5-8.5, and 22 points were selected along the Vietnamese coastline, out of which 10 points yielded proper values (non-NaN) that are shown in Figure 6 (Bruun parameter points). The allocation of a Bruun parameter point to a specific beach was performed via the AGP software's "spatial join" analysis tool and match option "closest geodesic", which means that every beach obtained its Bruun parameter values from the Bruun parameter point closest to it.

The SLR data are from the CMIP6 and are projected with respect to 1995 – 2014. The SLR ranges are between 0.054 and 0.401 m for SSP1-1.9, between 0.097 and 0.4565 m for SSP1-2.6, between 0.231 and 0.5795 m for SSP2-4.5, and between 0.3415 and 0.6965 m for SSP3-7.0 and 0.439 and 0.791 m for SSP5-8.5 along the Vietnamese coasts, respectively (Figure 7).

The smallest SLR value was from Bruun parameter point 3 (Figure 6). However, all other values from point 3 were acceptable and were approximately the same magnitude as the values from other points, which is why the point was included despite its small SLR values.

The wave data was extracted from the WAVEWATCH III (WW3) model's global 30 min dataset with 0.5-degree latitude–longitude resolution from 1979 – 2009 (Tolman, 2009) because of the limited availability of future wave projection data along the Vietnamese coastline. Figure 8 and Figure 9 show the results of the wave data, and H_s and T_s are the average significant wave height and wave period, respectively, over the 30-year period. $H_{e,30}$ *and* $T_{e,30}$ are the significant wave height and wave period exceeding 12 hours over 30 years, respectively. H_s and $H_{e,30}$ ranged between 0.61 m and 1.42 m and between 2.13 m and 9.18 m, respectively. The highest H_s and $H_{e,30}$ values were found in the central area (south central coast), and the lowest values were found in the northern and southern (Mekong River Delta) areas. Each beach and point on the coastline (for the CVI analysis) was given the SLR and wave data at the closest point (Figure 6) to it. $H_{e,30}$ value of 9.18 m is high, but it is still well within the maximum wave height value found in the South China Sea (Naseef and Kumar, 2019).

The mean tidal range is shown in Figure 12 and is from AVISO+ and the fine element solution (FES) tidal model developed from 2014 – 2016, with a gridded resolution of 1/16°. The mean tidal range values range between 0.65

m and 4.92 m. The lowest values are in the southern Mekong River Delta region provinces next to the Gulf of Thailand and in the northern central coastal provinces, and the highest values are likewise in the southern Mekong River Delta region provinces but on the seaside side of South China and in the northeast coastal province Quanh Ninh.

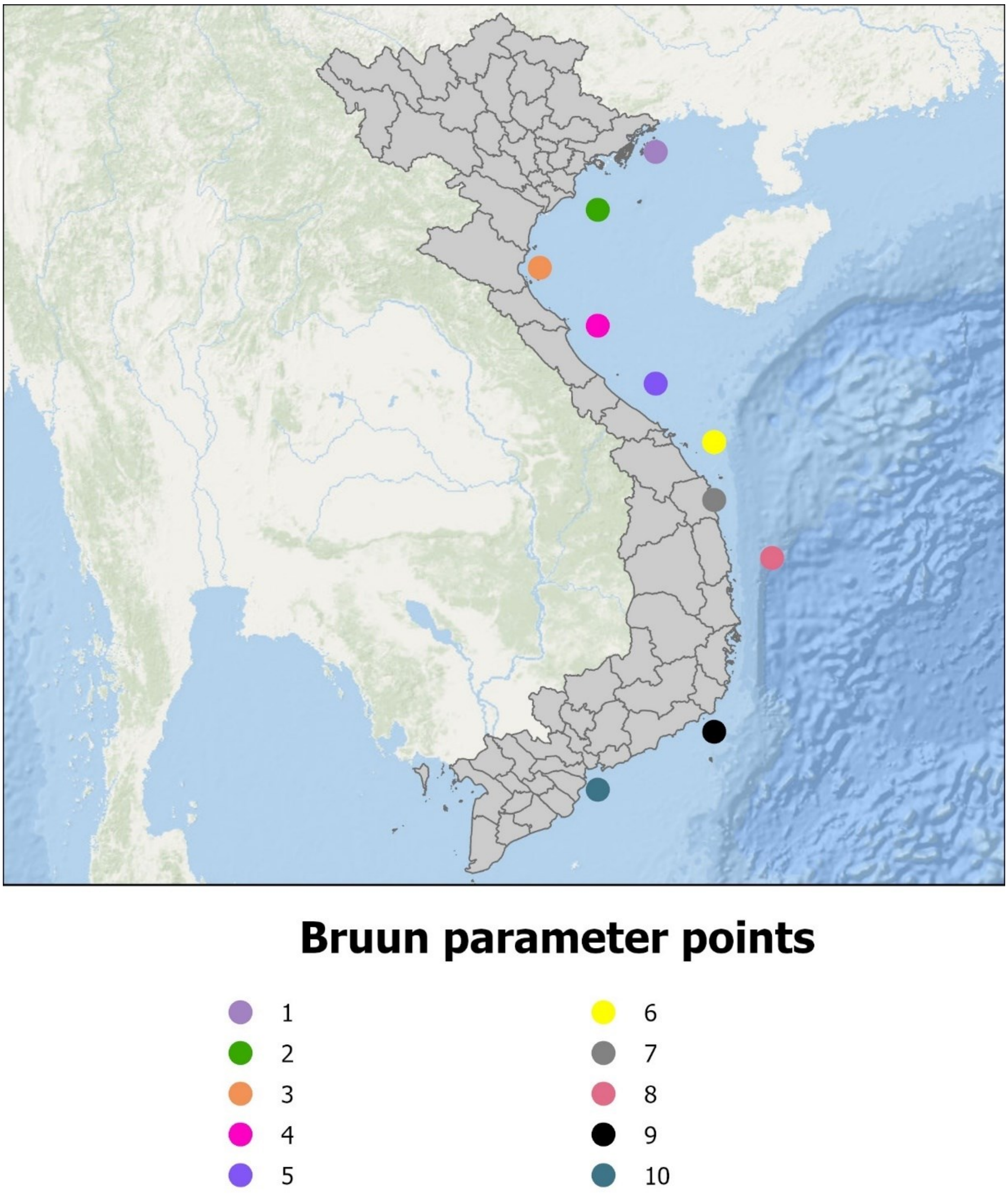

Figure 6 Bruun parameter points and their values were both used in the Bruun rule calculations.

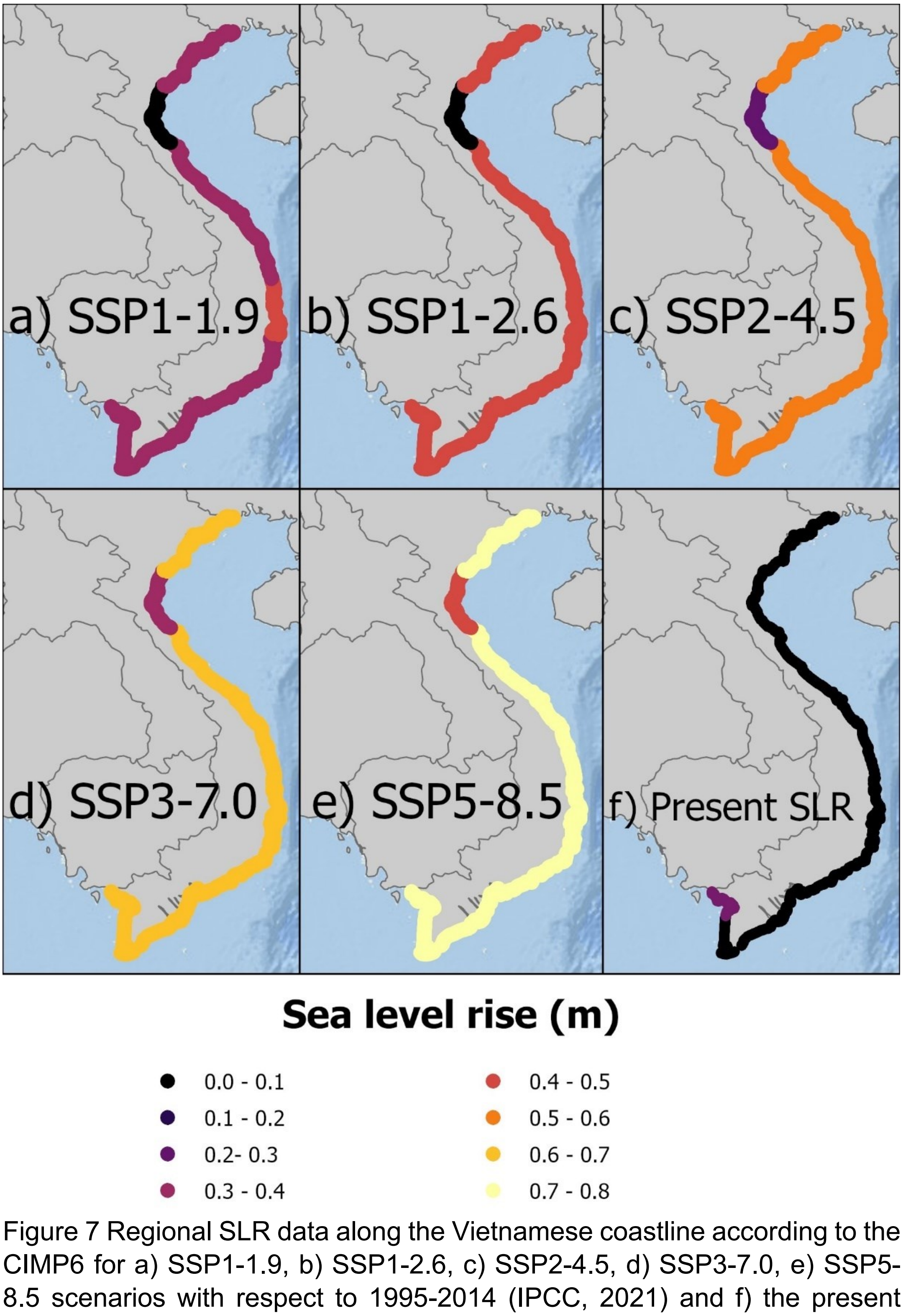

Figure 7 Regional SLR data along the Vietnamese coastline according to the CIMP6 for a) SSP1-1.9, b) SSP1-2.6, c) SSP2-4.5, d) SSP3-7.0, e) SSP5-8.5 scenarios with respect to 1995-2014 (IPCC, 2021) and f) the present (2010 – 2023) SLR.

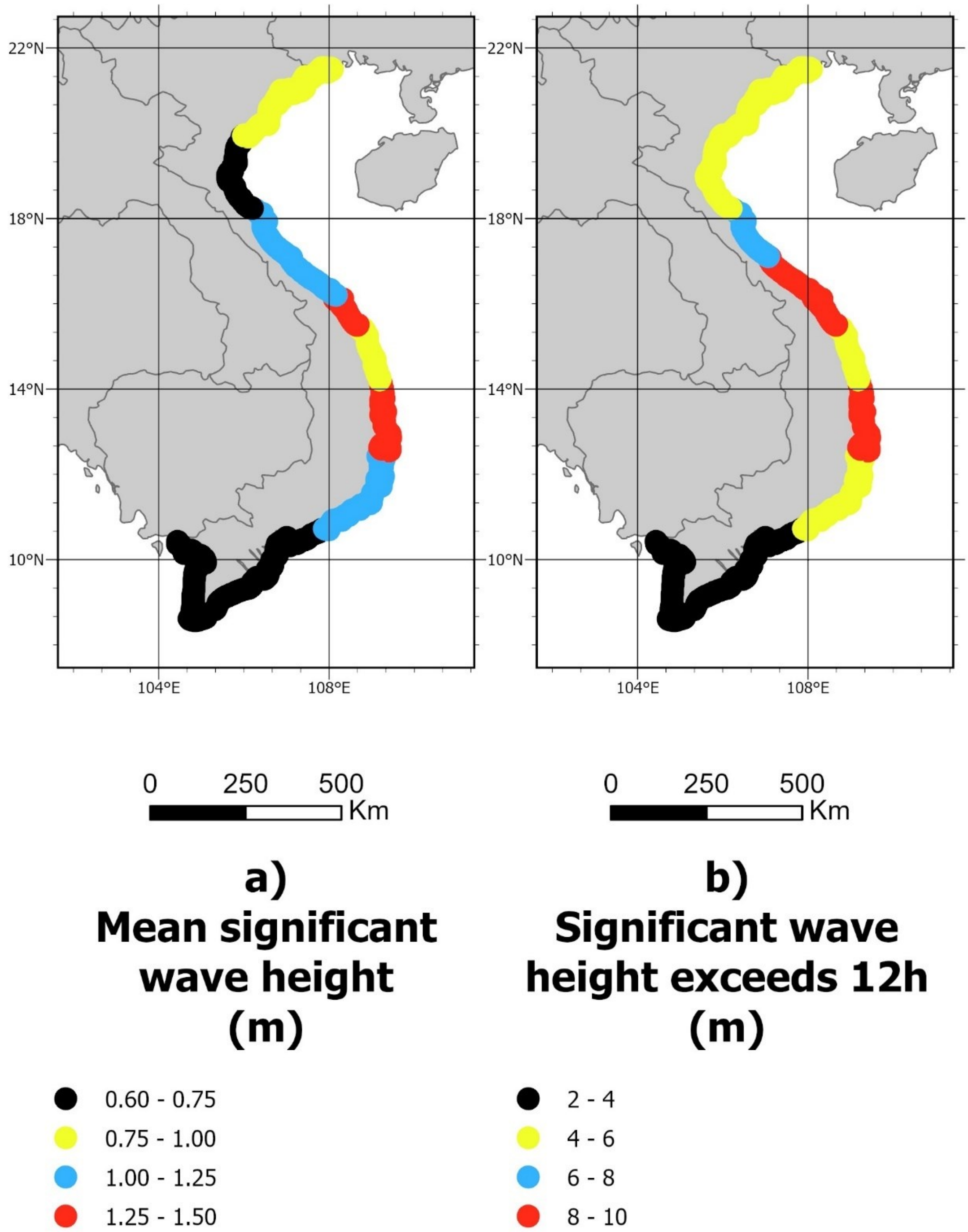

Figure 8 Reanalysis wave data from the WW3 model (Tolman, 2009) along the Vietnamese coastline 1989 – 2009: (a) H_s, (b) $H_{e,30}$ in meters.

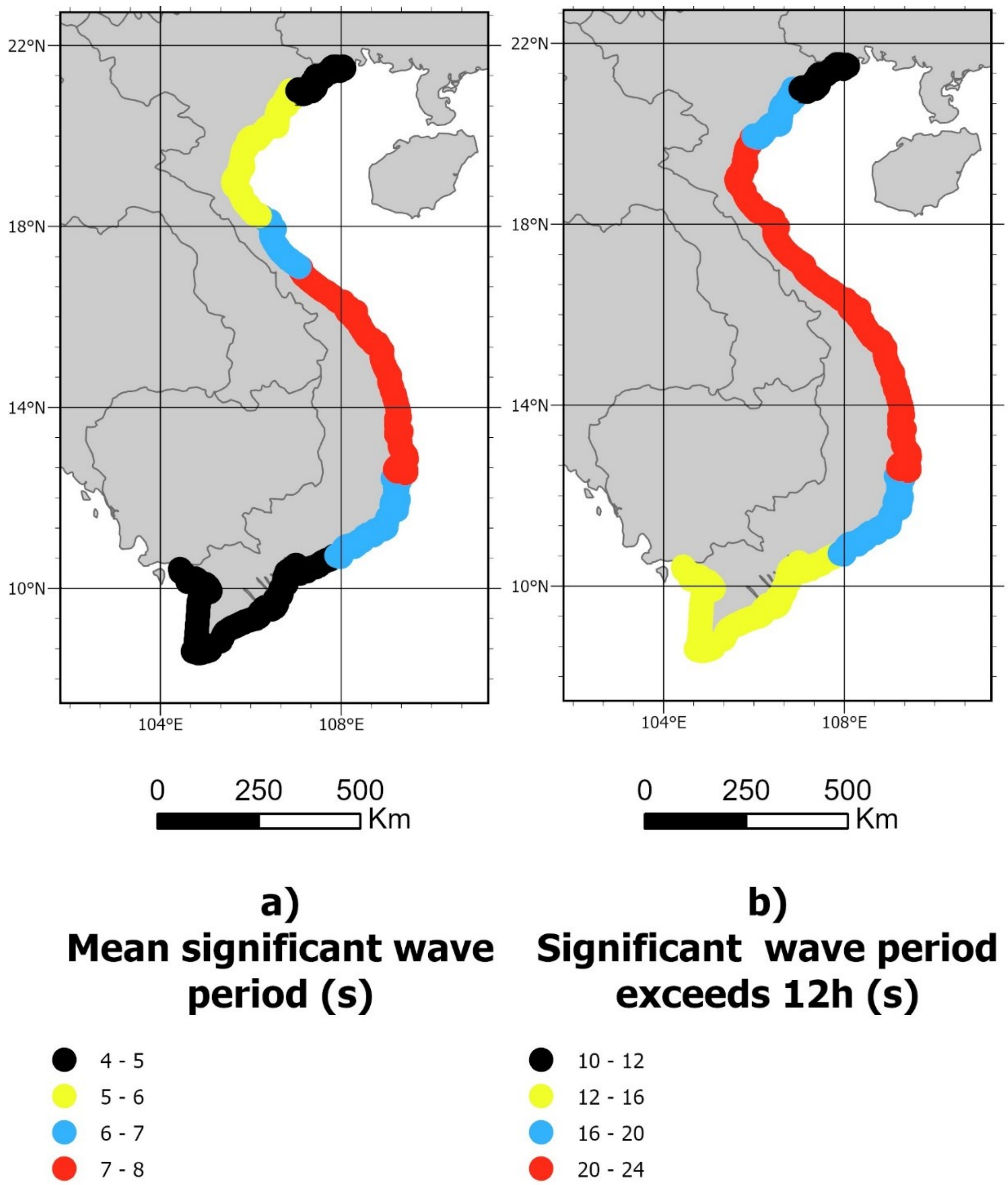

Figure 9 Reanalysis wave data from the WW3 model (Tolman, 2009) along the Vietnamese coastline 1989 – 2009: (a) T_S, (b) $T_{e,30}$ in seconds.

3.4 Coastal vulnerability index (CVI) against SLR methods

The CVI analysis used here is based on the ”National Assessment of Coastal Vulnerability to Sea-Level Rise: Preliminary Results for the Atlantic Coast” (1999) by the United States Geological Survey ((USGS), United States Geological Survey, 1999). The CVI was calculated via equation (6) by giving each if the 6 parameter its unique range of limits to allocate the values into 5 different classes which was based on either quantiles or previous research. The breakdown of CVI classes, values, ranges and their descriptions can be found in Table 1. The CVI results for present and future cases are shown in Figure 17.

$$CVI = \sqrt{\frac{a * b * c * d * e * f}{6}} \tag{6}$$

a) SLR
b) Slope
c) Erosion
d) Mean tidal range (MTR)
e) Mean significant wave height (MSWH)
f) Storm surge

Table 1 The CVI parameters, classes, descriptions and ranges. Sea level rise (SLR), significant wave height (SWH)

Vulnerability classes	Very low (1)	Low (2)	Moderate (3)	High (4)	Very high (5)
SLR (m)	<0.12	-	=0.439	-	> 0.7
Slope (-)	> 0.19	0.13 - 0.19	0.09 - 0.13	0.06 - 0.09	< 0.06
Erosion (%)	< 20	20 - 40	40 - 60	60 - 80	> 80
Mean tidal range (m)	< 0.60	1.60 - 1-75	1.75 - 3.00	3.00 - 3.30	> 3.30
Mean SWH (m)	< 0.40	0.40 - 0.50	1 - 1.2	0.90 - 1.30	> 1.30
Storm surge (m)	< 0.35	0.35 - 0.50	0.50 - 0.80	0.80 - 0.90	> 0.90

Table 2 CVI class distribution limits used for the results from Eq. (6)

CVI class	CVI calculations results
Very low	<7
Low	7-11
Moderate	11-13
High	13-16
Very high	16-36

The dataset source for the present SLR is (Copernicus Climate Change Service, Climate Data Store, 2018) and is from 2010 – 2023. It has global ocean horizontal coverage with a resolution of 0.25° × 0.25°. Its temporal coverage starts from Jan 1, 1993, to present with a latency of approximately 5 months. The means of the values were calculated over the study period (monthly data). The present SLR values range from 0.077 m to 0.103 m.

The legend scale is unified with the other SSP scenarios in the graph to make the comparison easier. The present SLR dataset only contains the SLR value and not the mean sea level. The values were low compared with the future SLR values, which is why all the present SLR values were given class 1 ("very low") values in the CVI analysis.

The future SLR dataset SSP5-8.5 (Figure 7) had 0.439 m as the smallest value, and the remaining values (upper limit) ranged from 0.772–0.791 m. As a result, the lowest value was assigned to class 3, and the remaining values were assigned to class 5 since breaking the upper limit values into more classes over a 0.19 m difference was deemed unnecessary. Therefore, the future SLR parameter in the CVI calculations only had classes 3 and 5 as possible values.

The present erosion loss percentages were calculated on the basis of the present SLR dataset. When the percentages of Bruun rule erosion, both present and future, calculated in this study were converted into CVI classes, the points along the Vietnamese coastline that did not have a beach in them or in their near vicinity (within a 1 km circle around the point to consider the differences in different dataset point locations) were given class 1 ("very low"). This was because the Bruun rule is not suitable for estimating shoreline retreat in non-beach areas. The basis for erosion limits was "equal interval" method in AGP.

Slope is a beach parameter that does not change rapidly over time, and the mean tidal range is due to astronomical bodies, which is why these parameters were assumed not to change within the next 100 years. The slope value limits (Table 1) were adopted from the paper by Ahmed et al. (2022). The mean tidal range was also based on “quantile” method in AGP.

The mean significant wave height (MSWH) and storm surge are expected to change, and datasets are available for future projections for both. The future MSWH dataset is a 140-year (1961–2100) climate simulation from two CMIP6 GCMs under the SSP1-2.6 and SSP5-8.5 scenarios with point locations every 10 degrees globally, and the dataset has a 0.5-degree global grid resolution. (Alberto et al., 2024). The MSWH data is from the years 2090 – 2100. SSP5-8.5 projections were used to match the Bruun rule erosion projections. The basis for SWH’s limits in Figure 10 was “quantile” in AGP for the future SWH values as it had larger range.

The present and future storm surge values are projections of the global storm surge dataset by Shimamura et al. (2022). The future data is based on the RCP8.5 scenario. This dataset contains the global annual maximum storm surge in the seamless experiment. It has a resolution of 0.1875°, which is approximately 20 km at low latitudes. The globe is composed of 2.4 million grid points with 2 km (coastal) and 25 km (deep ocean) spatial resolutions via the Advanced CIRCulation model (ADCIRC) version 55. The timeframe of the experiment is from 1950 – 2099. The present storm surge data is from 2010–2023, and the future storm surge data is from 2080–2099. This dataset was the only one available that extended all the way to 2099, which is the same as the IPCC’s SSP scenarios, and this dataset contained the maximum storm surge values. Therefore, the values from this dataset were used for both present and future cases to ensure that the values would be comparable to each other. The basis for the storm surge limitations in Figure 11 was “quantile” method in AGP.

The ranges for the present and future MSWH are shown in Figure 10. Their ranges are 0.61–1.42 m for the present and 0.27–1.46 m for the future. The maximum storm surge values are shown in Figure 11. Their ranges are 0.22–1.21 m for the present and 0.18–1.15 m for the future. The limits in Table 2 were used to categorize MSWH and storm surge into 5 different classes for CVI analysis. The basis for the categorization was considering the ranges together for present and future MSWH and the “quantile” method in AGP.

The class distribution in Table 2 was based on the quantile distribution of the future CVI calculation results. The present case CVI class values range from 1.22 – 7.91, and the future case values range from 2.58 – 35.36. SLR, erosion and SWH parameters future datasets are based on the SSP5-8.5 scenario and the storm surge future dataset is based on the RCP8.5 scenario.

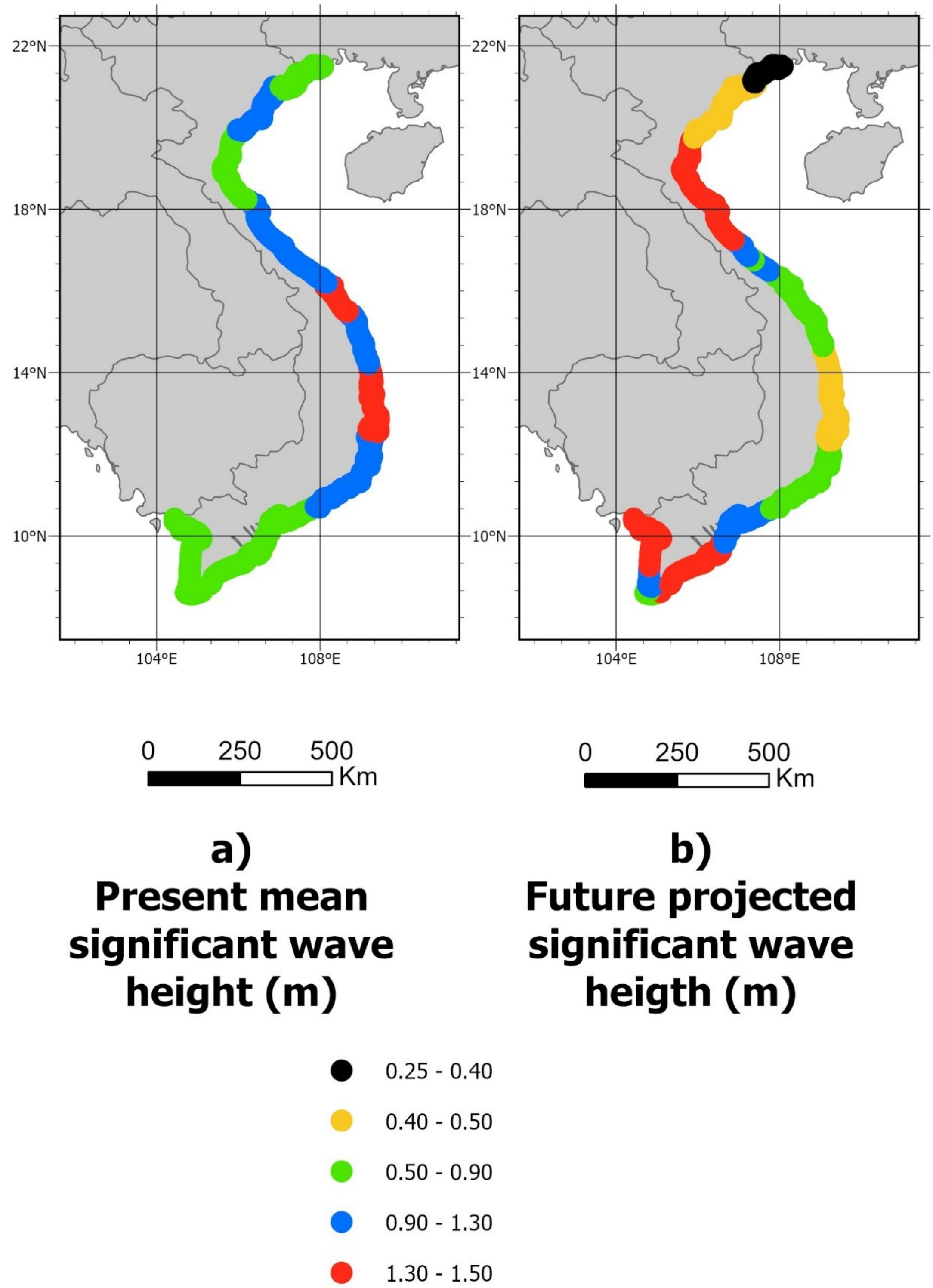

Figure 10 Comparison of the present and future mean significant wave heights

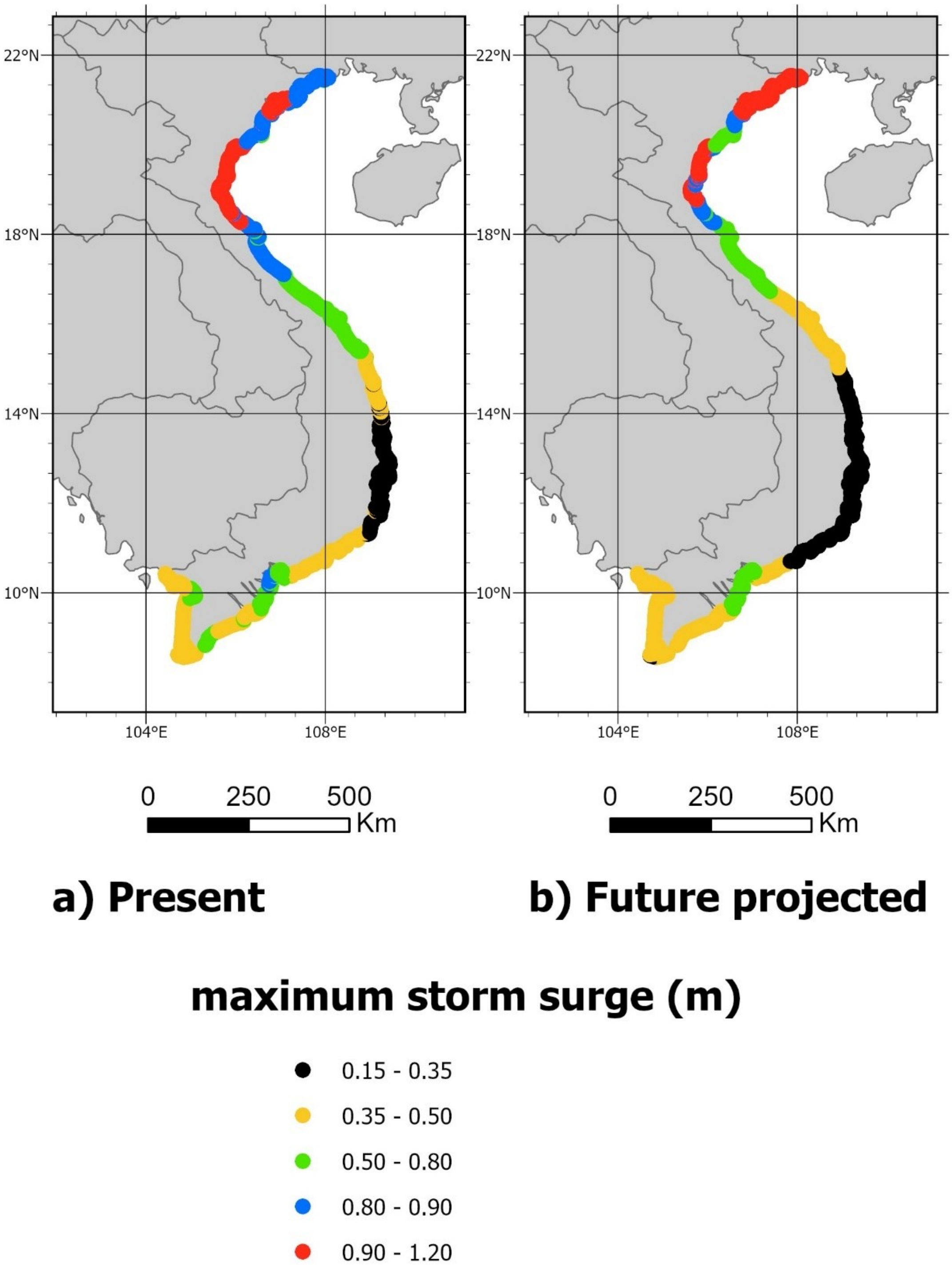

Figure 11 Comparison of the present and future maximum storm surges. The future data is based on the RCP8.5 scenario.

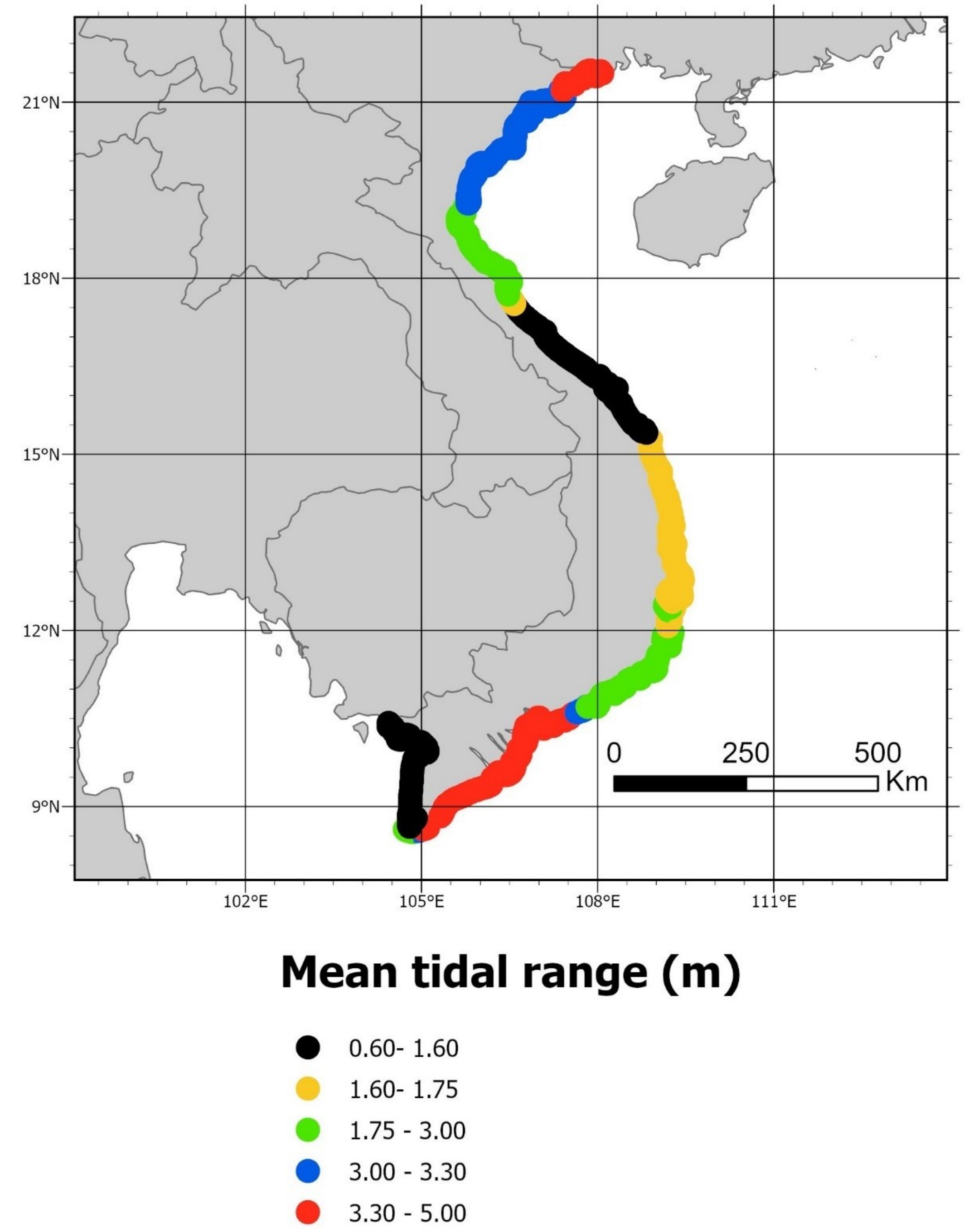

Figure 12 The mean tidal range (m) along the Vietnamese coastline

4 Results

4.1 Characteristics of sandy beaches

Figure 13 shows the beach width along the Vietnamese coast. More than 90% of the beach widths are less than 80 m from the total beaches in this study. There are 98 beaches whose beach width is greater than 80 m (Figure 13), and out of those, only 20 have a beach width greater than 150 m or greater. The percentages (less than 20 m, less than 80 m, and less than 400 m) in Figure 13 are 51.6%, 41.4% and 7.1%, respectively.

The total length of existing sandy beaches is 1330.1 km, which is 40.8% of the total coastline length. The total area of the sandy beaches was calculated to be 105.4 km^2. This was obtained by multiplying the corrected beach width (after performing the tidal correction) and longshore beach length and summing the areas. The provinces with the greatest percentages of sandy beaches (beach width) are Quang Ninh, Khan Hoa and Binh Thuan at 23.2%, 14.5% and 14.4%, respectively. The three provinces with the most sandy beaches are Ha Tinh, Quang Binh and Binh Tuan at 12.5%, 12.5% and 11.0%, respectively (Figure 13).

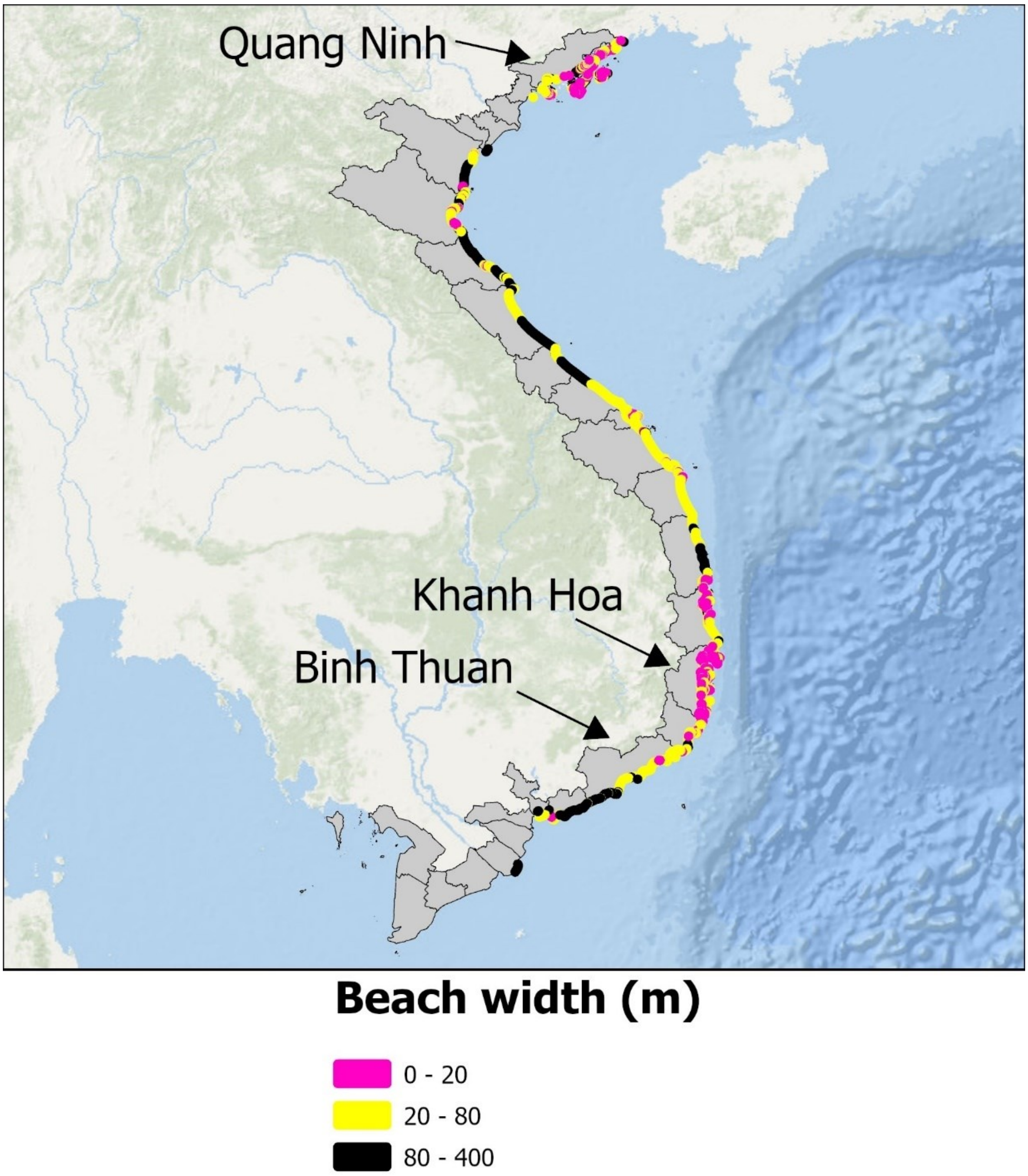

Figure 13 Beach width along the Vietnamese coast

4.2 Beach loss projections due to SLR

Figure 15 shows the beach loss projections (2081 – 2100) for every SSP scenario due to SLR along the Vietnamese coast. The total projected beach loss percentages were approximately 43% and 45.8 km^2 for SSP1-1.9, 49% and 51.1 km^2 for SSP1-2.6, 58% and 61.0 km^2 for SSP2-4.5, 63% and 66.5 km^2 for SSP3-7.0, and 67% and 70.6 km^2 for SSP5-8.5, respectively. Figure 14 represents the beach loss percentage for the present (2010 – 2023) SLR. It was used in the present CVI calculations, and a comparison with Figure 15 provides an estimate of how the situation will change in the future.

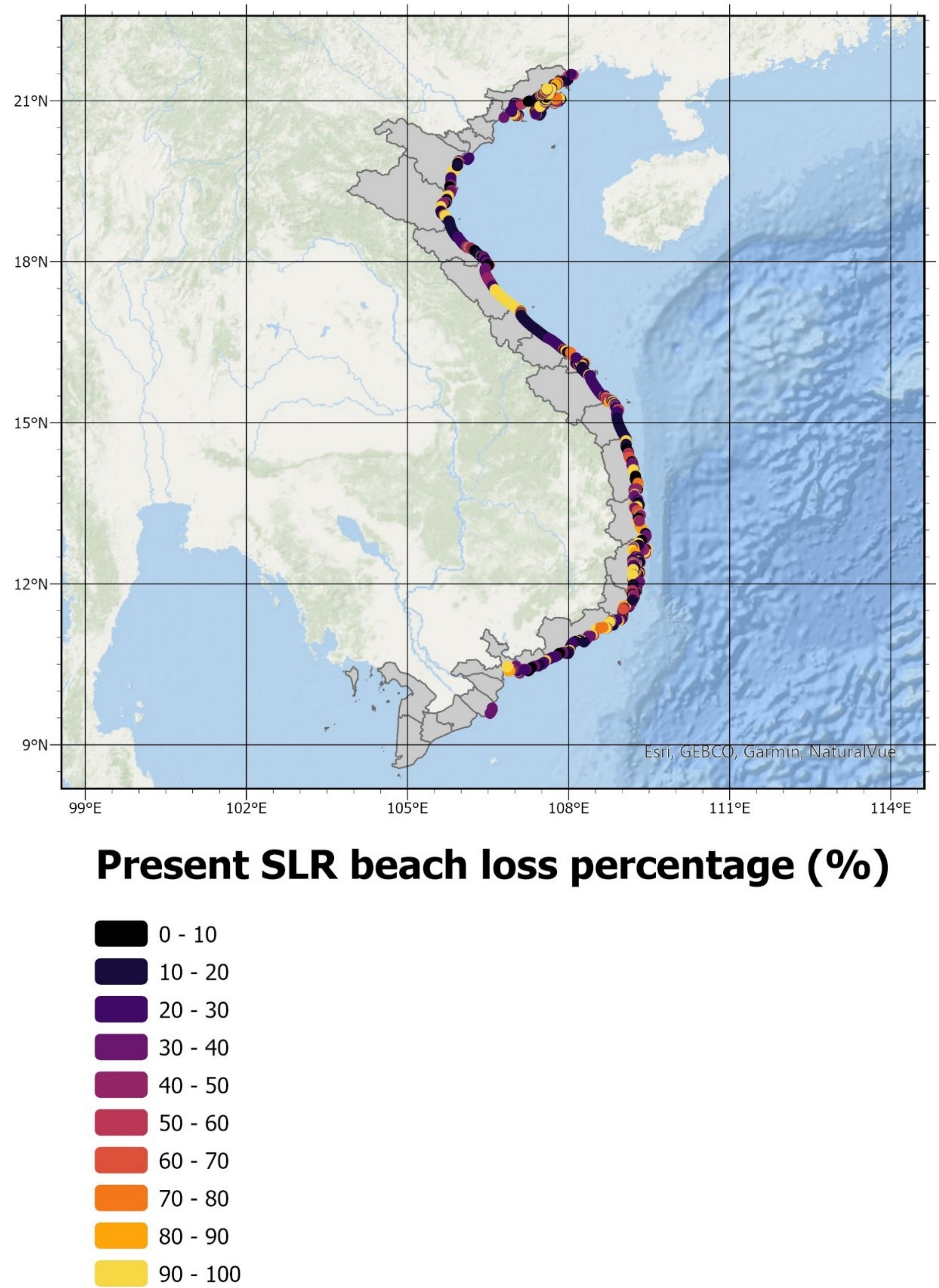

Figure 14 Present percentages of sea level rise beach loss

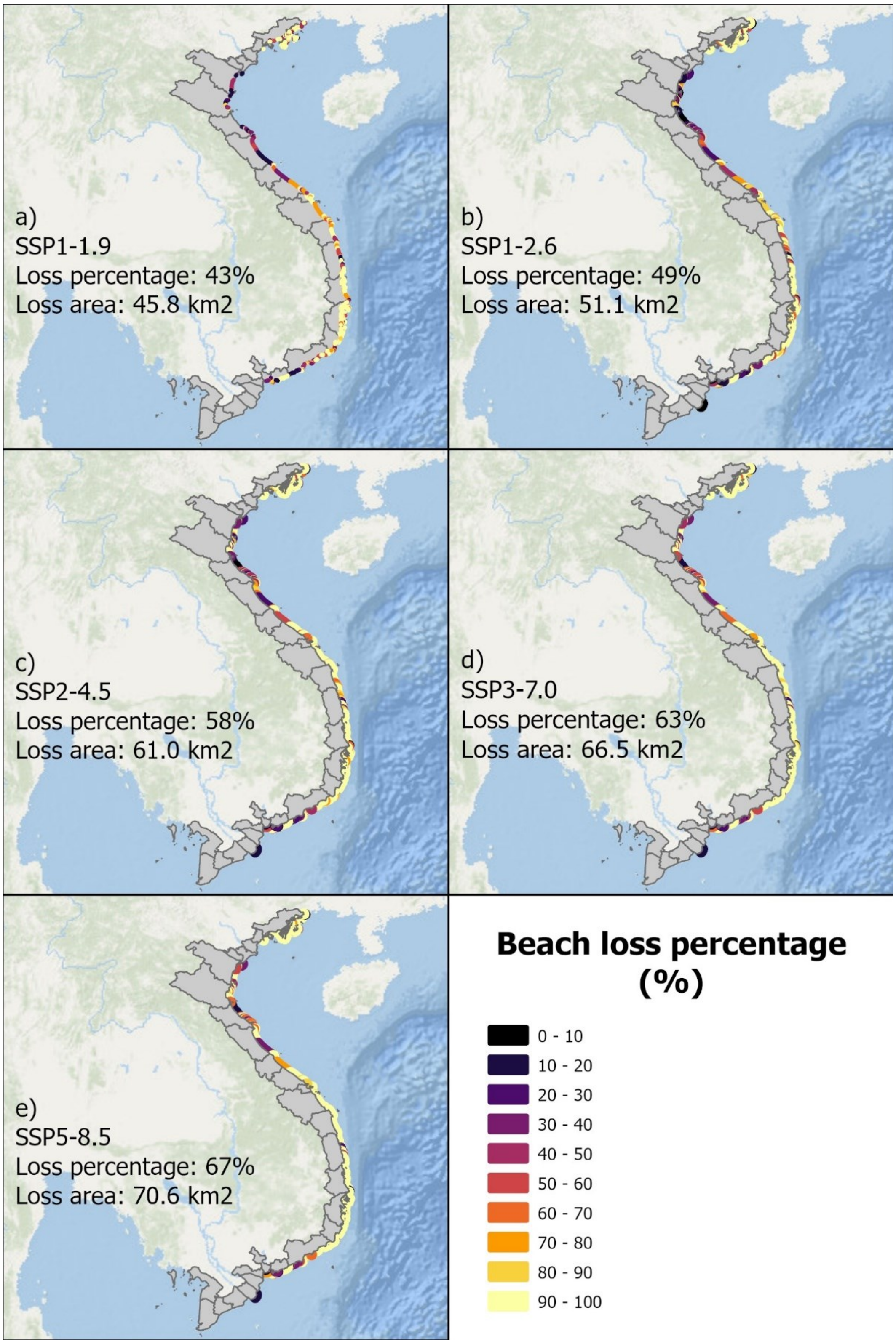

Figure 15 Projections for future beach loss percentages and areas relative to the reference period 1995-2014 based on regional SLR data for five SSP scenarios of the CMIP6.

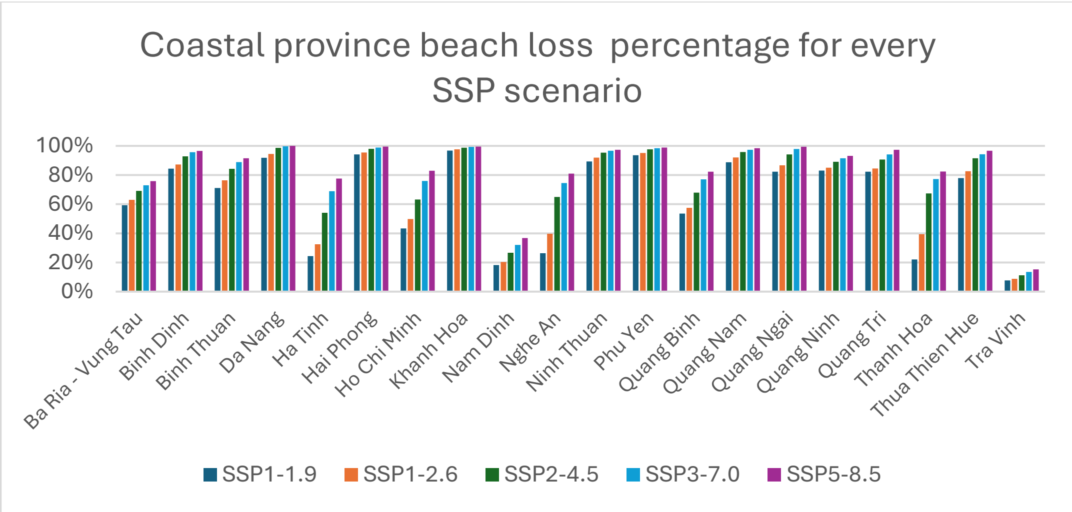

Figure 16 Coastal province beach loss percentage for every SSP scenario

Figure 16 highlights the beach loss percentage for every coastal province for every SSP scenario. For the SSP1-1.9 scenario, the greatest percentages of beach loss occurred in Khanh Hoa, Hai Phong and Phu yen at 97%, 94% and 94%, respectively.

For the SSP5-8.5 scenario, the provinces with the highest percentages of beach loss were Da Nang, Khanh Hoa and Hai Phong at 100.0%, 99.5% and 99.5%, respectively. The provinces with the greatest increases in the beach loss percentage under the different SSP scenarios are Thanh Hoa, Ha Tinh and Nghe An, with increases of 274%, 218%, and 207%, respectively. The lowest increases are observed in Khanh Hoa, Hai Phong, and Phu Yen, with 2.8%, 5.6%, and 5.7% increases, respectively.

4.3 Coastal vulnerability index (CVI) against SLR results

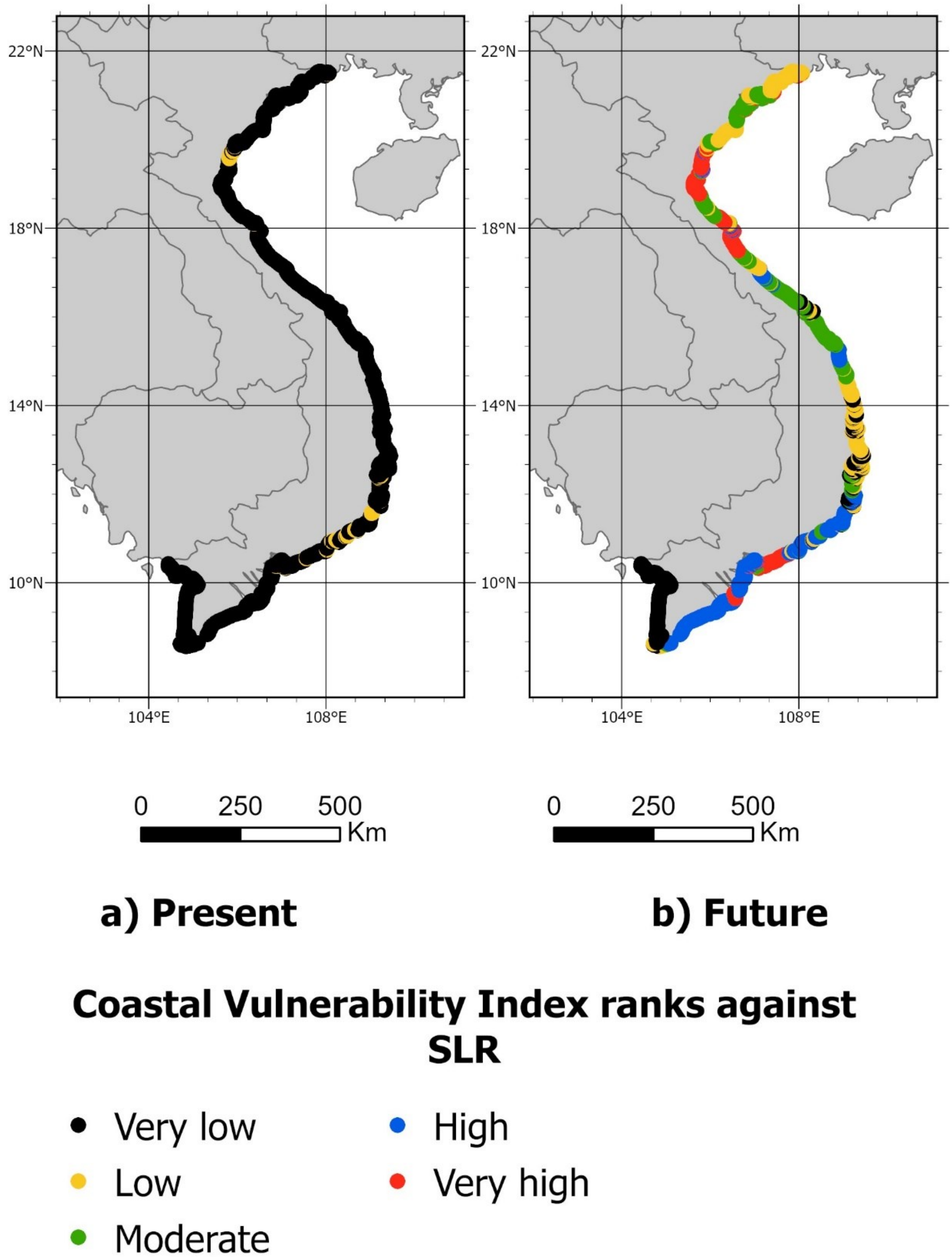

Figure 17 CVI results for present and future cases and their descriptions

The class distributions for the present and future cases are presented in Table 3. The present case is practically only the “very low” class. For the future case, there are roughly the same number of “low” (27.5%) and “moderate” (27.4%) classes. The remaining three classes are approximately evenly distributed in terms of magnitude at 17.0%, 14.7% and 13.4%, respectively.

Table 3 CVI class distribution percentages for the present and future cases.

CVI class	Present	Future
Very low	97.1%	17.0%
Low	2.9%	27.5%
Moderate	0.0%	27.4%
High	0.0%	14.7%
Very high	0.0%	13.4%

The present case’s “low” classes are located mainly in the southeastern area of the Vietnamese coastline, and a few classes are in the northern area (Figure 17). At these points, the SLR and storm surge classes are all “very low”. Slope and erosion have basically only classes that are “very high”. The mean tidal range (MTR) has classes from “moderate” to “very high”, and the significant wave height (SWH) has only classes “moderate” and “high”.

For the future case, the “very low” classes are located mainly on the southern central coast and in the Mekong River Delta area (Figure 1). SLR has only classes that are “very high”. For erosion, the class “very low” makes up 95% of the points. Sixty-nine percent of the slope classes are class “very high”, and for MTR, the classes “very low” and “low” make up 89% of the total points. For storm surge, 44% of the points and the “very low” and “low” classes make up the remainder of the points. For SWH, classes “High” and “Very high” make up 49% of the points.

The future case class “very high” is in the northern part of Vietnam’s coastline, mainly in the North Central Coast part (Figure 1). The SLR class “very high” makes up 72% of the points, while the rest are “moderate”. For the slope, the class “very high” holds 96% of the points. In total, 68% of the erosion classes are classified as “very high”. The MTR classes “High” and “Very high” account for 65% of the points. For SWH, the class “very high” makes up 68% of the points. For storm surge, the classes “High” and “Very high” make up 58% of the points.

The “low” class points (2.9%) in the present CVI case (Table 3) mapped out in the following way in the future CVI: 9% mapped into the “moderate” class, 41% mapped into the “high” class, and the remaining 50% of them mapped into the “very high” class. The “very low” class points (17.0%) in the future CVI case (Table 3) were all in the same class as those in the present CVI case.

5 Discussion

5.1 The results in a broader context

The findings from this study are presented along with (Xiao et al., 2023) findings about China in Table 4. Xiao et al. (2023) studied future beach loss projections in China via the Bruun rule. The total beach areas for Vietnam and China are 105.4 km^2 and 104.9 km^{2,} respectively. The results are similar in percentage values. Vietnam experiences more beach loss under the SSP1-1.9, SSP1-2.6 and SSP2-4.5 scenarios, whereas China experiences more beach loss under the SSP3-7.0 and SSP5-8.5 scenarios.

Xiao et al. (2023) compared the beach loss projections for representative concentration pathway (RCP) and SSP scenarios and reported that the differences in beach loss rates for global mean SLR (GMSLR) under the RCP and SSP scenarios are insignificant. Monre (2016) investigated the SLR scenarios for Vietnam's coastline, and the SLR amounts were similar between the RCP scenarios (2.6, 4.5, 6.0, and 8.5) and the SSP scenarios (2.6, 4.5, 7.0 and 8.5). The SSP1-1.9 scenario is excluded from this comparison because it has no counterpart with respect to the RCP scenarios. On the basis of the reasons above, the comparison of SSP scenarios for Vietnam and RCP scenarios for Egypt, Japan and Thailand seems reasonable.

The numbers in Table 5 are from Sharaan and Udo (2020) for Egypt, Udo and Takeda (2017) for Japan and Ritphring et al. (2018) for Thailand. Vietnam's beach losses are greater under scenarios 2.6, 4.5 and 6.0/7.0, whereas Thailand's area is greater under scenario 8.5 (Table 5). Egypt's beach losses are less than half of those of Vietnam under the 2.6, 4.5, and 6.0/7.0 scenarios and slightly greater than half of Vietnam's beach losses but overall still less than those of Vietnam under the 8.5 scenario (Table 5). Compared with Japan, Vietnam experiences less beach losses under every scenario. Japan experiences between 10% and 16% more beach losses depending on the scenario (Table 5).

Table 4 Future beach loss projections for Vietnam and China under the five SSP scenarios. The numbers for China are from Xiao et al. (2023).

	Vietnam (%)	China (%)
SSP1-1.9	43 %	39 %
SSP1-2.6	49 %	44 %
SSP2-4.5	58 %	56 %
SSP3-7.0	63 %	66 %
SSP5-8.5	67 %	71 %

Table 5 Future beach loss projections for Vietnam (SSP), Egypt (RCP), Japan (RCP) and Thailand (RCP) under different scenarios. The numbers are from Sharaan and Udo (2020) for Egypt, Udo and Takeda (2017) for Japan and Ritphring et al. (2018) for Thailand.

Scenario	Vietnam (%)	Egypt (%)	Japan (%)	Thailand (%)
2.6	49 %	22 %	62 %	46 %
4.5	58 %	26 %	71 %	55 %
6.0/7.0	63 %	26 %	73 %	57 %
8.5	67 %	36 %	83 %	72 %

The total cross-shore length (the sum of each beach width) of the Vietnamese sandy beaches was calculated to be 44.6 km. The loss of beach width was obtained by summing the shoreline retreats calculated via the Bruun rule for every SSP scenario. The total projected beach width loss percentages were approximately 62% and 27.7 km for SSP1-1.9, 66% and 29.5 km for SSP1-2.6, 74% and 33.0 km for SSP2-4.5, 79% and 35.1 km for SSP3-7.0, and 82% and 36.5 km for SSP5-8.5, respectively, of the total beach width. This resulted in losses of beach width per beach of 19.9 m SSP1-1.9, 21.2 m SSP1-2.6, 23.7 m SSP2-4.5, 25.3 m SSP3-7.0 and 26.3 m SSP5-8.5. For the SSP5-8.5 scenario in the study area, the median shoreline retreat was 19.0 m (out of the individual shoreline retreat values of the 1390 beaches).

Athanasiou et al. (2020) estimated that the average SLR-driven median shoreline retreat in Europe would be 97 m for the RCP8.5 scenario and 54 m for the RCP4.5 scenario by year 2100 relative to the baseline year 2010. They included the whole European coastline, not only sandy beaches, and their scale was at the continental level, which is why the results are larger than those for only Vietnam’s coastline.

5.2 Uncertainties, limitations and the way forward

Further research into the erosion situation is needed in Vietnam. The addition of more tidal measurement points and improving long-term measurement data could decrease the number of uncertainties in the future. The beaches were collected manually in AGP via visual inspection, which means that beaches could have been missed because of poor satellite imagery quality or high tide blocking the entire beach.

When performing the tidal correction, there were only four tidal measurement points along the entire Vietnamese coastline, which resulted in each beach being given the mean tidal level from the tidal measurement point closest to it. Furthermore, owing to the lack of long-term data from two of the tidal measurement points up north, their tide values had to be approximated by the South Central Coast point via coefficients.

Multiple slope values could have been chosen for the beaches in the dataset by Athanasiou et al. (2023) (Figure 18). The coastal slope was chosen over the other two slopes because storm surge is considered a variable in the CVI calculations; thus, having the sandy area of the beach until the first peak (coastal max) be a part of the beach slope was deemed beneficial. The global slope dataset by Athanasiou et al. (2023) contained 4411 slope values for the entire Vietnamese coastline after clipping. Owing to the beach slope and sediment size connection reported by Wiegel (1992), this number decreased to 1774 (40.2% remaining) since the acceptable range for the slope is between 0.01 and 0.2. The 1 km spacing between the transects in the dataset could also have affected the beach slope values.

Acceptable SLR values were obtained from only 10 out of the 22 points located along the Vietnamese coastline. The dataset for SLR (IPCC, 2021) had a resolution of 0.5 degrees, which limited the possible Bruun parameter point locations as well.

The Bruun rule has had its share of criticism over the years as a way to project beach loss in the future due to SLR. Cooper and Pilkey (2004) stated that the Bruun rule has unrealistic assumptions, such as (a) the equilibrium profile describes the shape of the shoreface, (b) the sediment balance is zero, and (c) waves are the only cause of all sand movement on the shoreface. However, when performing large-scale, long-term projections, the Bruun rule is a simple and viable computational method to help grasp the future erosion situation.
The AGP program tool “Minimum Bounding Geometry” was used to obtain a rough estimate of every beach width. Furthermore, when calculating the total length of sandy beaches along the Vietnamese coastline, every beach was

assumed to be a rectangle. The area of a beach divided by the beach width provides an estimate of the alongshore length of the beach. The sum of all the beaches' alongshore lengths was used as the total sandy beach length along the Vietnamese coastline.

The 6 parameters used in the CVI calculations have their own ranges and based on the ranges, their own classes too (Table 1). This means that the parameter values affect the results only if their variation is large enough to increase or decrease the class of the parameter. The degree to which a parameter value can vary before it affects the class of the parameter differs among the 6 parameters. The slope has the smallest variation range (0.01–0.182), and erosion has the largest variation range (0–100%).

The CVI results were also divided into 5 different classes (Table 2). Changes in the CVI results can have no effect as long as the change is small enough so that the CVI result stays in the same class. The "moderate" class has the smallest range at 11 – 13, and the "very high" class has the largest range at 16 – 36.

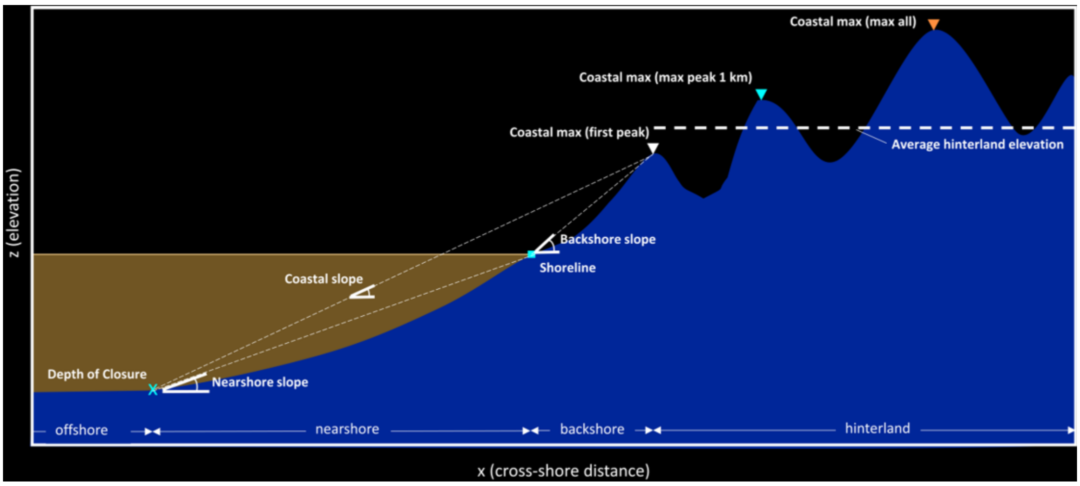

Figure 18 Three different beach slope values presented in the paper by Athanasiou et al. (2023).

5.3 Adaptation Measures for Future Beach Loss

Vietnamese mangroves provide coastal protection from storm events, in addition to being productive and biologically important ecosystems worldwide. This regional importance of mangroves, especially in the Red River Delta region, is due to the ecosystem services (coastal protection) that they provide. However, these mangroves have been lost in recent decades (~38%) or degraded due to conversion to aquaculture and coastal development or during the war in Vietnam. This degradation has slowed recently because of restoration and protection measures. (Veettil et al., 2019).

The local government has policies for using mangroves for coastal protection and livelihood improvements; a good example of this is what they have already done in Kien Giang Province in southern Vietnam. Mangrove rehabilitation also has potential as a soft climate change adaptation strategy for mitigating the impacts of coastal storms and SLR in Vietnam. (Veettil et al., 2019). However, mangroves are not suitable for the protection of sandy beaches, as they exist mainly behind beaches that protect areas even further inland.

Hard structures, such as breakwaters, dikes and seawalls, have been used throughout the world for coastal protection from SLR. In Vietnam, the hard structures used include concrete walls, rocky barriers and sea dikes.
Bioshields such as mangrove forests, nearshore-coral reefs and marshes and seagrass meadows have also become viable options worldwide for long-term coastal protection. Compared with hard structures, the maintenance and restoration of bioshields (mangrove forests) can be a cost-effective way to mitigate coastal hazards. (Veettil et al., 2021).

In the future, the ecoengineering concept, which involves the combination of hard structures and natural ecosystems, could help Vietnam gain more opportunities from coastal protection, tourism development and economic stability perspectives. (Veettil et al., 2021).

Upon visual inspection of the beaches in this study along the Vietnamese coastline in the AGP, these structures protect other coastal structures (harbors, river mouth areas or entrances to canals) rather than sandy beaches. There were a few occasions when a beach was partially covered by an adjacent hard structure, but sandy beach protection was not the primary target of the structure. This means that most of the sandy beaches found in this study were basically unprotected.

Currently, different kinds of hard structures are used to prevent coastal erosion in Vietnam. However, bioshields (mangrove forests) could be a more cost-effective way to mitigate coastal hazards. Ecoengineering concepts could become a viable way to protect the Vietnamese coastline in some areas.

6 Conclusions

In this study, sandy beaches along the Vietnamese coastline were collected, and their locations, lengths and widths were recorded. Their future beach loss projections due to SLR at the end of this century over a national scale under different SSP scenarios were calculated via the Bruun rule.
The results indicate that the Vietnamese coastline has a total beach length of 1330.1 km. Along the coastline, Quang Binh, Ha Tinh and Binh Thuan Provinces have the highest percentages of sandy beaches area wise, with 13%, 13% and 11%, respectively. The worst-case projections along the Vietnamese coast show future beach losses of 67% and 70.6 km^2 for the SSP5-8.5 scenario in CMIP6. Severe beach losses of more than 90% are projected along the South Central Coast provinces.
What is new in this study is the combination of future erosion projections and adaptations along the entire Vietnamese coastline. These findings, combined with CVI analysis for present and future cases, provide new information about the state of the Vietnamese coastline. According to the Bruun rule projected erosion results, the erosion situation will worsen, ranging from 43% and 45.8 km^2 of the total sandy beach area lost in the SSP1-1.9 scenario to 67% and 70.6 km^2 of the total sandy beach area lost in the SSP5-8.5 scenario.
Research has not been conducted before on the future erosion projections along the entire Vietnamese coastline, which is why this study was conducted. The current adaptation methods for beach erosion are based on hard structures and some mangroves. In the future, ecoengineering solutions could help Vietnam gain more opportunities from coastal protection, tourism development and economic stability perspectives. This study can help policy makers in Vietnam assess future needs for coastal protection measurements in coastal provinces.

References

Ahmed, M.A., B. Sridharan, Nilanjan Saha, S.A. Sannasiraj, S.A. Sannasiraj, 2022. Assessment of coastal vulnerability for extreme events. Int. J. Disaster Risk Reduct. 82, 103341. https://doi.org/10.1016/j.ijdrr.2022.103341

Alberto, M., Young, Ian, Trenham, Claire, Hemer, Mark, 2024. CMIP6 global wind-wave 21st century climate projections - combined. http://hdl.handle.net/102.100.100/601698?index=1

Athanasiou, P., Ap van Dongeren, Alessio Giardino, Michalis I. Vousdoukas, Roshanka Ranasinghe, Jaap Kwadijk, 2020. Uncertainties in projections of sandy beach erosion due to sea level rise: an analysis at the European scale. Sci. Rep. 10, 11895. https://doi.org/10.1038/s41598-020-68576-0

Athanasiou, P., Ap van Dongeren, Maarten Pronk, Alessio Giardino, Michalis Vousdoukas, Roshanka Ranasinghe, 2023. Global Coastal Characteristics (GCC): a global dataset of geophysical, hydrodynamic, and socioeconomic coastal indicators. https://doi.org/10.5194/essd-16-3433-2024

Beatley, T., David Brower, Anna K. Schwab, 2002. An Introduction to Coastal Zone Management.

Bilkov, D.M., Molly M. Mitchell, Megan K. La Peyre, Jason D. Toft, 2017. Living Shorelines The Science and Management of Nature-Based Coastal Protection, 1st ed. CRC Press, Boca Raton.

Bird, E.C.F., 2008. Coastal geomorphology : an introduction, second edition. Wiley, Chichester, England.

Bruun, P., 1962. Sea-level rise as a cause of shore erosion. J. Waterw. Harb. Div. 88, 117–130.

Cooper, J.A.G., Pilkey, O.H., 2004. Sea-level rise and shoreline retreat: time to abandon the Bruun Rule. Glob. Planet. Change 43, 157–171. https://doi.org/10.1016/j.gloplacha.2004.07.001

Copernicus Climate Change Service, Climate Data Store, 2018. Sea level gridded data from satellite observations for the global ocean from 1993 to present. https://doi.org/DOI: 10.24381/cds.4c328c78 (Accessed on 15.08.2024)

Duc, D.M., Kazuya Yasuhara, Hieu M. Nguyen, Nguyen chau Lan, 2016. Climate change impacts in a large-scale erosion coast of Hai Hau District, Vietnam and the adaptation. J. Coast. Conserv. 48, 47–62. https://doi.org/10.1007/s11852-016-0471-7

Eric C. F. Bird, 1964. Coastal Geomorphology: An Introduction. Wiley.

F. P. Shepard, 1948. Submarine Geology. Harper & Row, New York.

Grove Karl Gilbert, 1890. Lake Bonneville. U.S. Geological Survey, Washington, D.C.

GSO [WWW Document], 2024. . Gen. Stat. Off. Vietnam. URL https://www.gso.gov.vn/en/homepage/ (accessed 8.30.24).

Hinkel, J., Robert J. Nicholls, Richard S.J. Tol, Zheng B. Wang, Jacqueline M. Hamilton, Gerben Boot, Athanasios T. Vafeidis, Loraine McFadden, Andrey Ganopolski, Richard J.T. Klein, 2013. A global analysis of erosion of sandy beaches and sea-level rise: An application of DIVA. Glob. Planet. Change 111, 150–158. http://dx.doi.org/10.1016/j.gloplacha.2013.09.002

IPCC, 2021. Climate change 2021: The physical science basis. Cambridge University Press, Cambridge, United Kingdom.

IPCC, 2019. Intergovernmental Panel on Climate Change (IPCC) Special Report on the Ocean and Cryosphere in a Changing Climate. Cambridge University Press.

Luijendijk, A., Hagenaars, G., Ranasinghe, R., Baart, F., Donchyts, G., Aarninkhof, S., 2018. The State of the World's Beaches. Sci Rep 8, 6641. https://doi.org/10.1038/s41598-018-24630-6

Monre, 2016. Ministery of Natural Resources and Environment, Summary for Policymakers. Ha Noi.

Naseef, T.M., Kumar, V.S., 2019. Climatology and trends of the Indian Ocean surface waves based on 39-year long ERA5 reanalysis data. Int. J. Climatol. 40. https://doi.org/10.1002/joc.6251

Nguyen, C.H., K. B. Dang, N. V. Liem, Van Bao Dang, Quang Hai Truong, Dang Hoi Nguyen, Tuan Linh Giang, Pham Thi Phuong Nga, Chi Cuong Ngo, Thi Thuy Hoang, Thi Ngoc Dang, 2021. New Approach to Assess Multi-Scale Coastal Landscape Vulnerability to Erosion in Tropical Storms in Vietnam. Sustainability 13, 1004. https://doi.org/DOI: 10.3390/su13021004

Nicholls, R.J., William A. Birkemeier,, Robert J. Hallermeier, 1996. Application of the Depth of Closure Concept. Coast. Eng. https://doi.org/10.1061/9780784402429.29

Pang, T., Wang, X., Nawaz, R.A., Keefe, G., Akedanmbi, T., 2023. Coastal erosion and climate change: A review on coastal-change process and modeling. Ambio 52, 2034–2052.

Prasad, D.H., Kumar, N.D., 2014. Coastal Erosion Studies—A Review. Int. J. Geosci. 5, 341–345. https://doi.org/10.4236/ijg.2014.53033

R. W. G. Carter, 1988. An Introduction to the Physical, Ecological, and Cultural Systems of Coastlines, Akademic Press. ed. London.

Ritphring, S., Nidhinarangkoon, P., Udo, K., Shiwakawa, H., 2021. The Comparative Study of Adaptation Measure to Sea Level Rise in Thailand. J Mar Sci Eng 9, 588. https://doi.org/10.3390/jmse9060588

Ritphring, S., Somphong, C., Keiko Udo, So Kazama, 2018. Projections of Future Beach Loss due to Sea Level Rise for Sandy Beaches along Thailand's Coastlines. J. Coast. Res. 85, 541–545. https://doi.org/10.2112/SI85-109.1

Schoonees, T., A. Gijón Mancheño, B. Scheres, T. J, Bouma, R. Silva, T. Schlurmann, H. Schüttrumpf, 2019. Hard Structures for Coastal Protection, Towards Greener Designs. Estuaries Coasts 42, 1709–1729. https://doi.org/10.1007/s12237-019-00551-z

Sharaan, M., Udo, K., 2020. Projections of future beach loss along the mediterranean coastline of Egypt due to sea-level rise. Appl. Ocean Res. 94, 101972. https://doi.org/10.1016/j.apor.2019.101972

Shimamura, T., W. J. Pringle, N. Mori, T. Miyashita, K. Yoshida, 2022. Seamless Projections of Global Storm Surge and Ocean Waves Under a Warming Climate. Geophys. Res. Lett. 49. https://doi.org/10.1029/2021GL097427

Somphong, C., Udo, K., Ritphring, S., Shiwakawa, H., 2020. Beach Nourishment as an Adaptation to Future Sandy Beach Loss Owing to Sea-Level Rise in Thailand. J Mar Sci Eng 8, 659. https://doi.org/10.3390/jmse8090659

Sunamura, T., 1983. Coastal and beach changes by waves. Trans. Jpn. Geomorphol. Union 4, 179–188.

Takeda, I., Sunamura, T., 1983. Formation and spacing of beach cusps. Coast. Eng. Jpn. 26, 121–135.

Thinh, N.A., Nguyen Ngoc Thanh, Luong Thi Tuyen, Luc Hens, 2018. Tourism and beach erosion: valuing the damage of beach erosion for tourism in the Hoi An World Heritage site, Vietnam. Environ. Dev. Sustain. 21, 2113–2124. https://doi.org/10.1007/s10668-018-0126-y

Tolman, H.L., 2009. User manual and system documentation of WAVEWATCH III TM version 3.14.

Udo, K., Takeda, Y., 2017. Projections of Future Beach Loss in Japan Due to Sea-Level Rise and Uncertainties in Projected Beach Loss. Coast. Eng. J. 59, 1740006-1-1740006–16. https://doi.org/10.1142/S057856341740006X

U.S. Army Corps of Engineers, 2002. Coastal Engineering Manual. Washington D.C.

(USGS), United States Geological Survey, 1999. National Assessment of Coastal Vulnerability to Sea-Level Rise: Preliminary Results for the Atlantic Coast. US Geol. Surv. Open-File Rep. 99–593.

Veettil, B.K., Raymond D. Ward, Ngo Xuan Quan, Ngo Thi Thu Trang, Tran Hoai Giang, 2019. Mangroves of Vietnam: Historical development, current state of research and future threats. Estuar. Coast. Shelf Sci. 218, 212–236. https://doi.org/10.1016/j.ecss.2018.12.021

Veettil, B.K., Raymond D. Ward, Nguyen Thi Kim Dung, Dong Doan Van, Ngo Xuan Quang, Pham Ngoc Hoai, Nhat-Duc Hoang, 2021. The use of bioshields for coastal protection in Vietnam: Current status and potential. Reg. Stud. Mar. Sci. 47, 101945. https://doi.org/10.1016/j.rsma.2021.101945

Vinh, B.T., Truong, N.H., 2012. EROSION MECHANISM OF NGA BAY RIVERBANKS, HO CHI MINH CITY, VIETNAM. ASEAN Eng. J. 3, 132–141. https://doi.org/10.11113/aej.v3.15530

Vousdoukas, M.I., Roshanka Ranasinghe, Lorenzo Mentaschi, Theocharis A. Plomaritis, Panagiotis Athanasiou, Arjen Luijendijk, Luc Feyen, 2020. Sandy coastlines under threat of erosion. Nat. Clim. Change Vol. 10, 260–263. https://doi.org/10.1038/s41558-020-0697-0

Wiegel, R.L., 1992. Oceanographical Engineering. Dover Publications, Inc., New York.

Williams, S.J., K. Dodd, KK Gohn, 1991. Coasts in Crisis. U.S. Geological Survey.

Xiao, S., Udo, K., Zhang, Y., 2023. Projections of future beach loss along the Chinese coastline due to sea level rise. Coast. Eng. J. 65, 620–637. https://doi.org/10.1080/21664250.2023.2265683